Front. Energy 2022, 16(5): 747–773
https://doi.org/10.1007/s11708-022-0830-z

REVIEW ARTICLE

Shuwei ZHANG, Liyan SHANG, Zhen PAN, Li ZHOU, You GUO

Mechanism and control factors of hydrate plugging in multiphase liquid-rich pipeline flow systems: a review

Abstract There is nothing illogical in the concept that hydrates are easily formed in oil and gas pipelines owing to the low-temperature and high-pressure environment, although requiring the cooperation of flow rate, water content, gas-liquid ratio, and other specific factors. Therefore, hydrate plugging is a major concern for the hydrate slurry pipeline transportation technology. In order to further examine potential mechanisms underlying these processes, the present paper listed and analyzed the significant research efforts specializing in the mechanisms of hydrate blockages in the liquid-rich system, including oil-based, water-based, and partially dispersed systems (PD systems), in gathering and transportation pipelines. In addition, it summarized the influences of fluid flow and water content on the risk of hydrate blockage and discussed. In general, flow rate was implicated in the regulation of blockage risk through its characteristic to affect sedimentation tendencies and flow patterns. Increasing water content can potentiate the growth of hydrates and change the oil-water dispersion degree, which causes a transition from completely dispersed systems to PD systems with a higher risk of clogging. Reasons of diversity of hydrate plugging mechanism in oil-based system ought to be studied in-depth by combining the discrepancy of water content and the microscopic characteristics of hydrate particles. At present, it is increasingly necessary to expand the application of the hydrate blockage formation prediction model in order to ensure that hydrate slurry mixed transportation technology can be more maturely applied to the natural gas industry transportation field.

Keywords hydrate, flow rate, water content, mechanism of pipeline blockage, rich liquid phase system

Received Sept. 3, 2021; accepted Jan. 14, 2022; online Jun. 30, 2022

Shuwei ZHANG, Zhen PAN
College of Petroleum Engineering, Liaoning Petrochemical University, Fushun 113001, China

Liyan SHANG (✉)
College of Environmental and Safety Engineering, Liaoning Petrochemical University, Fushun 113001, China
E-mail: shangliyan@lnpu.edu.cn

Li ZHOU
College of Petrochemical Technology, Liaoning Petrochemical University, Fushun 113001, China

You GUO
Fushun City Special Equipment Supervision and Inspection Institute, Fushun 113001, China

1 Introduction

Natural gas hydrate is additionally known as “combustible ice” [1], which is a cage crystal formed by water molecules and gas guest molecules under low-temperature and high-pressure conditions [2,3]. The water molecules are related to each other through hydrogen bonds [4,5]. The guest molecules are surrounded by the water molecule lattices by van der Waals forces. Natural gas hydrates have many hidden uses, such as storage and transportation of natural gas [6,7], desalination [8,9], gas separation [10,11], cold energy storage [12,13], and carbon dioxide storage and capture [14,15], etc. However, natural gas hydrate is also a serious obstacle to the safe and stable transportation of natural gas from oil reservoirs to various gas processing sites. Outage owing to hydrate blockage can cause a great deal of economic losses and other serious consequences. In the Soviet Union, the phenomenon of hydrate blockage in transportation pipelines was discovered for the primary time [16], subsequently, hydrate blockage in oil and gas pipelines has become a hot spot for numerous scholars.

Long-term studies showed that formation of natural gas hydrate required certain temperature and pressure conditions [17]. The traditional blocking prevention and control method was heating pipeline or adding thermodynamic inhibitors to change the phase balance of hydrate formation, making it more difficult for the environment to satisfy conditions required for hydrate formation, and fundamentally preventing the formation of hydrates.

However, due to expensive economic cost, the traditional method was not generally applicable to pipeline prevention and control. There was an urgent sense that improvements must come from fresh approaches. Then, later generations developed a method of adding low-dose kinetic inhibitors and anti-aggregation agents or mixing the two in a certain ratio to prevent large amounts of hydrates from accumulating in a pipeline, so as to keep it flowing in the form of slurry in pipelines, which has achieved an excellent anti-blocking effect [18]. Different from the hydrate growth characteristics in a static environment, the hydrate generation state, post-generation morphological evolution, and flow characteristics in a flowing state affected the clogging process of pipeline hydrates [19,20]. So far, many scholars have observed the state and morphological characteristics of the hydrate formation in the reaction system through the visual microscope in the autoclave [21–23]. However, for the hydrate formation process and slurry flow characteristics in various systems in the flow loop, there is a lack of in-depth research and summary.

Hydrate flow systems were divided into liquid-rich systems and gas-rich systems according to the main transport medium. According to the water content of the liquid phase and the gas-liquid flow rate, the liquid-rich systems can be further divided into oil-based, water-based, and partially dispersed systems (PD systems) [24]. Pipeline blockage in the liquid-rich systems was affected by many factors, such as temperature, pressure, water content, oil phase type, gas-liquid ratio, and additives. These factors can affect the accumulation and deposition, the viscosity of the slurry, the induction time, and the final production volume of hydrates in the oil-water emulsion, which caused different pipe blockage mechanisms and blockage risks. In-depth understanding of the influence of various factors on the flow and blockage characteristics of the hydrate slurry can improve the blockage prevention and control in the actual pipeline transportation field. At present, there are few reports on the clogging mechanism in the gas-rich systems. Therefore, scholars are strengthening the research in this field. The research on the flow and plugging characteristics of hydrates in the rich liquid system mainly comes from the experiment results of loop which belong to Colorado School of Mines, China University of Petroleum, Beijing, University of Western Australia, and China University of Petroleum. The present paper which combined studies in these institutions on the hydrate blockage process in the liquid-rich system and research on the influence of various factors on the flow and clogging characteristics of hydrate slurry, summarized the mechanisms of hydrate pipe blockage in the liquid-rich systems, and explored in-depth the influence trend of water content and flow rate on the risk of hydrate slurry pipe blockage in order to provide certain theoretical support for the safe transportation field of the natural gas industry and the hydrate blockage risk control system.

2 Blocking process of hydrates in oil and gas pipelines

The process of hydrate blockage in rich-liquid systems generally include hydrate formation, aggregation and pipe wall deposition, and pipe blockage. First, hydrates are formed at the gas-water interface. The hydrates formed are initially dispersed in the liquid phase and continue to grow, and the hydrate particles eventually aggregate under the action of the capillary liquid bridge force. Thereafter, the hydrates continue to grow and hydrate aggregates are also increasing, eventually inflicting blockage owing to hydrate deposits in the pipeline. The main process is shown in Fig. 1. Therefore, after the formation of hydrates, perhaps the accumulation of particles and the deposition on the pipe wall were the two major causes of hydrate blockage. In this section, the research on the aggregation and deposition mechanisms of hydrate particles are sorted out.

2.1 Mechanism of hydrate aggregation

There are agglomeration and separation forces between particles. The agglomeration forces include the van der Waals force F_{vw}, the capillary liquid bridge force F_{cap}, and the electrostatic force F_e. The separation forces mainly include the collision force F_c, the shear force F_{shear}, and the aggregate gravity G and buoyancy F_v [26,27]. Figure 2

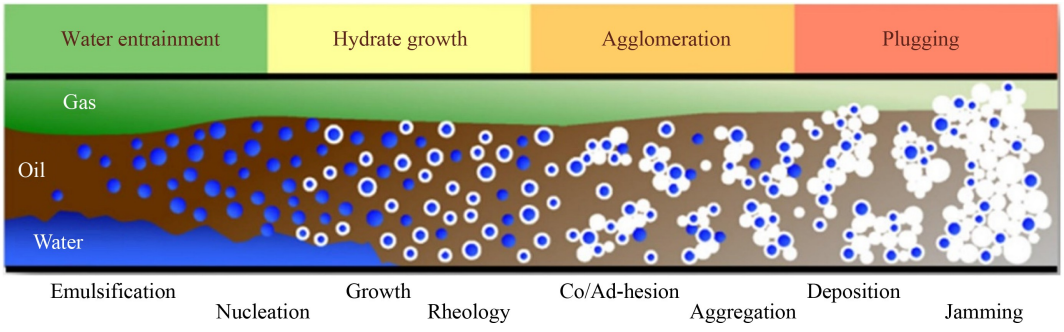

Fig. 1 Conceptual diagram of hydrate blockage in oil and gas pipelines (adapted with permission from Ref. [25]).

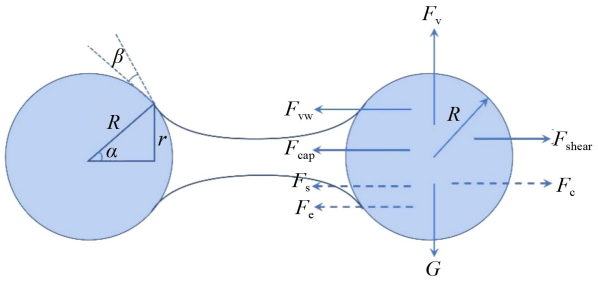

Fig. 2 Schematic diagram of agglomeration and separation forces between hydrate particles (α is the contact angle and β is the semi-filled angle (adapted with permission from Ref. [24]).

depicts the force analysis between hydrate particles when agglomeration occurs. Numerous studies have shown [28,29] that the numerical magnitude of the aggregation force between particles is the same as that of the capillary liquid bridging force, which is much larger than other aggregation forces. Therefore, the aggregation force between the hydrate particles is dominated by the capillary liquid bridging force which is calculated by using Eq. (1) [30].

$$F_{cap} = 2\pi R_a \gamma_{II} \cos\theta, \tag{1}$$

where R_a is the radius of the hydrate particles, γ_{II} is the interfacial tension, and θ is the contact angle between the liquid bridge and the surface of the hydrate particles. The annealing in the tube wall can cause the liquid bridge between the hydrate particles to solidify and become a fixed bridge. Correspondingly, the liquid bridge force will also become a more stable fixed bridge force F_s [31]. At this stage, the bridge force between particles can be calculated by using Eq. (2) [32].

$$F_s = \tau_t A, \tag{2}$$

$$A = \pi r^2 = \pi (R \sin\varphi)^2, \tag{3}$$

where τ_t is the tensile strength of pure hydrate, and A is the cross-sectional area of the fixed bridge, which can be calculated by using Eq. (3), where φ is the fill angle, and R is the radius of particles. One of the fundamental assumptions in the study of hydrate aggregation is the aggregation between hydrate particles. However, Palermo et al. [33] had different opinions for particle aggregation, who proposed that the reason for hydrate aggregation was not the interaction between hydrate particles, but the binding reaction between hydrate particles and water droplets. The contact between natural gas hydrate and water droplets induced the conversion of water droplets into hydrate particles, resulting in hydrate particle aggregation. Currently, there is no key microscopic evidence on these aspects to prove the aggregation process between hydrate particles. It is, therefore, necessary to further study the mechanism of hydrate aggregation.

2.2 Mechanism of hydrate deposit

According to Refs. [34–36], bedding, tube wall film growth, and tube wall adhesion of hydrate particles are considered to be three major mechanisms of hydrate deposition in pipelines. The macro characteristics of the three mechanisms and the reasons for their formation are summarized and analyzed in Table 1.

2.2.1 Hydrate bedding

Hydrate particle bedding generally refers to the process of hydrate particle sinking to the bottom of the tube under the action of gravity (if the density of the hydrate is lighter than fluid, the hydrate is at the top of the tube), thereby forming a fixed hydrate bed [37–40]. Under normal circumstances, hydrate particles with high concentration, large particle size, and low flow velocity are more likely to form bedding sedimentary layer. The solid-liquid flow pattern of the pipeline during the entire bedding and deposition process experienced four stages [41]. The processes are shown in Fig. 3, in which Fig. 3(a) is the uniform suspension flow. In the initial stage of hydrate formation in the pipeline, the volume fraction of particles is small, the particles can be evenly distributed in the liquid phase, and the system maintains a stable flow. Figure 3(b) is the non-uniform suspension flow. With the continuous generation of hydrate, the number and volume fraction of hydrate particles in the pipeline increase, so does the particle size due to aggregation and growth. Therefore, the fluid flow rate decreases. The hydrate particles begin to unevenly distribute in the liquid phase, and the particle concentration at the bottom of the pipeline increases. Figure 3(c) is the moving bed laminar flow. The flow rate continues to decrease, the hydrate

Table 1 Three major mechanisms of hydrate deposition

Deposition mechanism	Implantation deposition	Tube wall film growth	Tube wall adhesion
Macro characteristics	A process in which numerous hydrate particles settled to the bottom or top of the pipe under the action of gravity to form a fixed bed of hydrates	After the medium in the pipe contacts the pipe wall, the hydrates are formed on the pipe wall and grew into a film	After the hydrate is generated inside the flow field and contacts with the pipe wall, hydrate particles stay on the pipe wall through the adhesion force with the pipe wall
Main reasons for formation	High concentration of hydrate particles, large particle size, and low fluid flow rate	There is a temperature gradient between the fluid in the pipe and the pipe wall, which causes the medium to diffuse from the center of the pipe to the pipe wall	Capillary liquid bridge force and van der Waals force

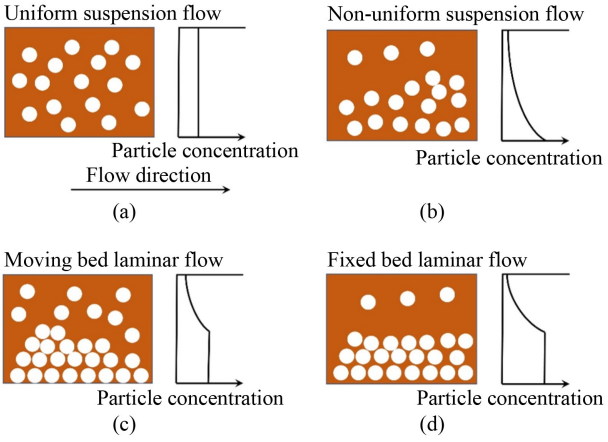

Fig. 3 Schematic diagram of four processes of hydrate implantation and deposition (adapted with permission from Ref. [41]).
(a) Uniform suspension flow; (b) non-uniform suspension flow; (c) moving bed laminar flow; (d) fixed bed laminar flow.

particles sink down under the action of gravity, and the moving bed formed by the hydrate particles begins to appear at the bottom of the pipeline. Figure 3(d) is the fixed bed laminar flow. With continuous subsidence of the hydrate particles, the height of the bed rises and the moving speed gradually decreases until it comes to a stop. At this time, the moving bed is completely transformed into a fixed bed.

2.2.2 Wall film growth of hydrate

The growth of hydrate tube wall film generally refers to the process of forming hydrate and growing into a film on the tube wall after the medium in the tube contacts the tube wall. The growth of the hydrate film typically requires a metal tube wall with a lower temperature than that of the liquid phase in the tube to provide subcooling support. The main reason for the growth of the tube wall film is the temperature distinction between the fluid in the tube and the tube wall. This temperature difference causes the diffusion of the medium from the center of the tube with a higher temperature to the tube wall with a lower one. Related research shows that the temperature difference between the fluid and the pipe wall is the main driving force for the growth of hydrates [42]. The larger the temperature difference, the more it promotes the diffusion of hydrate molecules, the faster the hydrate film grows, the thicker the hydrate film forms, and the easier the pipeline blockage occurs. The growth of tube wall membrane, which is divided by different media diffusion modes, is confirmed in gas-dominated systems, water-dominated systems, oil-based systems, and the PD system. As demonstrated in Fig. 4, hydrate wall film growth dominated by gas molecular diffusion is a significant cause of hydrate film growth and deposition in water-dominated and PD systems. When there is a temperature gradient between the tube wall and the fluid, and the tube wall can provide a large degree of supercooling, the diffusion of the hydrate generating medium from inside the fluid to the tube wall can trigger the growth of the hydrate film of the water-dominated system. In a PD system, the oil phase brings some of the water phase to the tube wall to wet the surface of the tube wall, and the hydrate can form a hydrate film and grow after the tube wall has wettability. In the gas-based system and the oil-based system, the water phase exists in the form of free droplets, and the diffusion of water molecules dominates the formation of the tube wall film in these systems. In a gas-dominated system, the liquid droplets or steam form a liquid film on the pipe wall by splashing or condensation, and then the growth of hydrate starts at the gas-liquid-pipe wall interface, and spreads on the pipe wall through continuous growth to form a hydration film. The growth of the tube wall film in the

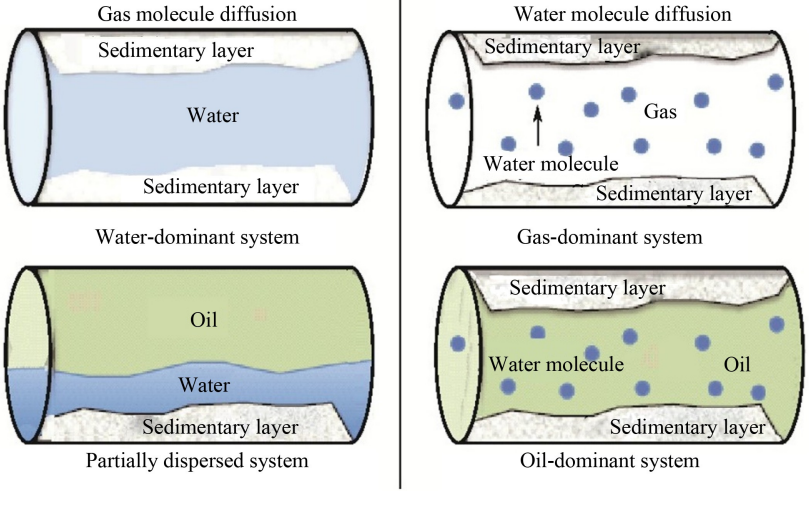

Fig. 4 Schematic diagram of hydrate film growth in four systems (adapted with permission from Ref. [42]).

oil-based system requires the wetting of the tube wall as a prerequisite, and a hydrate film is formed on the tube wall through the process of water molecule diffusion.

It is worth noting that although both the gas molecule diffusion and the water molecule diffusion are affected by the temperature difference between the fluid and the tube wall, the driving forces of the two are not the same. Water molecules diffuse from the fluid with a higher concentration to the tube wall with a lower one, while gas molecules diffuse from the fluid with a low solubility to the tube wall with a high concentration. The reason for this that the diffusion process of water molecules is driven by the concentration gradient, while the driving force for the diffusion of gas molecules is mainly the chemical potential gradient.

2.2.3 Wall adhesion of hydrate

The pipe wall adhesion process of hydrate particles generally means that after the hydrate generated inside the pipeline contacts with the pipe wall, hydrate particles can stay on the pipe wall by the adhesion force between the hydrate particles and the pipe wall. This adhesion force includes the electrostatic force, the capillary liquid bridge force, and the van der Waals force. Among these forces, the capillary liquid bridge force and the van der Waals force are the main ones promoting the adhesion of hydrate particles to the tube wall. When there is no water on the pipe wall and no external load on the particles, the van der Waals force is the main adhesion force. After the pipe wall is wetted, a liquid bridge is formed between the hydrate particles and the pipe wall. Because the negative pressure inside the liquid bridge can generate a strong capillary force, the capillary liquid bridge force becomes the main adhesion force [43]. After the tube wall hydrate deposit layer is annealed, the liquid bridges are converted into solid ones [32]. In general, the adhesion rate of the hydrate particles under the action of the solid bridge force is on the brink of 100%, and hydrate particles are difficult to remove under the action of their own flow. The schematic diagram of the mechanism of tube wall adhesion is exhibited in Fig. 5, in which φ is the contact angle, θ_1 and θ_2 are the contact angles of the sphere and the substrate, respectively.

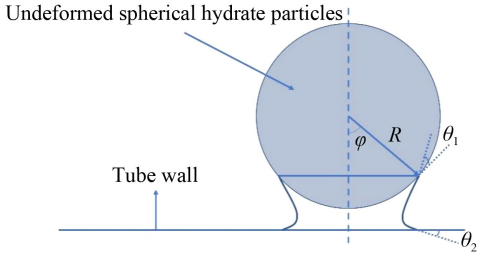

Fig. 5 Schematic diagram of mechanism of hydrate particles adhesion to tube wall (adapted with permission from Ref. [43]).

The van der Waals force (F_{vdw}) between the standard spherical hydrate particles and the tube wall can be expressed as

$$F_{vdw} = \frac{A_{12}R}{6z_0^2}, \tag{4}$$

where A_{12} is the Hamaker constant between sphere and substrate, R is the radius of the particle, and z_0 is the separation distance between the particle and the surface. When the wall surface is wetted, a liquid bridge is formed between the hydrate particles and the tube wall. The capillary liquid bridging force generated by the liquid bridge can cause the particles to condense with the tube wall. The capillary liquid bridging force with a smaller filling angle can be expressed as

$$F_{cap} = 2\pi R\gamma_1(\cos\theta_1 + \cos\theta_2), \tag{5}$$

where γ_1 is the surface tension of the liquid, while θ_1 and θ_2 are the contact angles of the sphere and the substrate, respectively. The calculation of the fixed bridge force formed owing to the solidification of the liquid bridge can refer to the calculation of the fixed bridge force between the hydrate particles in Eq. (2).

3 Mechanism of hydrates blockage in rich-liquid systems

3.1 Mechanisms of hydrate blockage in oil-based systems

In the early stage of mining, the water content of the mined product is comparatively low, resulting in a higher dispersion rate of water in the oil. Systems formed in this case is called oil-based systems. The oil-based systems contained oil, gas, and water phases with the oil phase as the dominant phase. Under the action of the oil phase, the majority of the water in the oil phase exist in the form of emulsified water droplets. The hydrate blockage mechanism in the oil-based system is the most diverse and complex. The aggregation of hydrate particles and the three hydrate deposition processes can cause pipeline blockage in the oil-based system. Turner of the Colorado School of Mines and Abrahamson of the University of Canterbury in New Zealand supported the speculation of blockage mechanism caused by hydrate accumulation. They proposed a mechanism of hydrate plugging in oil-based systems, which was accepted by most scholars [44]. The mechanism is displayed in Fig. 6. The hydrate blockage of oil-based systems can be divided into oil-water emulsification, hydrate shell growth, aggregation, and blockage.

In oil-water emulsification, under the action of various factors, most of the water in the system is dispersed in the continuous oil phase with the form of emulsified water droplets, and the whole system exists as a water-in-oil emulsion.

In hydrate shell growth, when the surrounding environment of the pipeline meets the conditions for hydrate

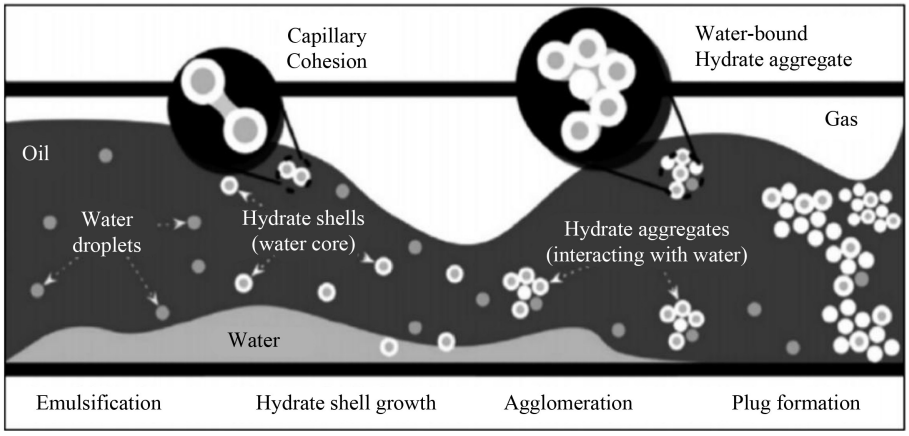

Fig. 6 Schematic diagram of mechanism of hydrates plugging in oil-based systems established by Turner et al. (adapted with permission from Ref. [45]).

formation, hydrates quickly forms at the oil-water interface, and the generated hydrates diffuses and surrounds the water droplets to form a hydrate shell. Turner et al. [45] believed that after the hydrate shell around the water droplets was formed, the hydrate continued to infiltrate into the water droplets and continuously grow. Therefore, the thickness of the hydrate shell continued to increase, and eventually the hydrate particles completed the infiltration process into the droplets or the growth was hindered by heat mass transfer process. The growth of the hydrate shell is presented in Fig. 7. Taylor et al. [46] also found that during the growth of the hydrate shell, the diameter of the formed hydrate particles is the same as that of the original water droplets until the end of the growth.

In aggregation, the initial form of hydrates exists as dispersed particles in the oil phase. As the hydrates continue to form, continuous coalescence occurs between hydrate particles or between hydrate particles and water droplets under the action of liquid bridging force, larger aggregates form which causes the deposition of hydrates in the pipeline. In blockage, eventually the hydrate aggregates settle in the pipelines and form blockages. Moreover, under the action of annealing, the hydrate film in the pipeline densifies, which increases the tendency of blockage in the pipeline.

With the widespread application and renewal of shaking reactors and experimental loops, scholars continue to propose new ideas for pipe blockage and deposition mechanisms in oil-based systems. Sum et al. [47] derived a deposition mechanism based on a wet solid surface. First, hydrates grow on the wet wall surface or at the phase interface and accumulate and deposit on the surface of the pipe wall, which leads to the fact that a hydrate deposit is formed on the pipe wall. Then, based on the original hydrate sediments, hydrates continue to grow to form a richer sedimentary layer, which eventually results in the obstruction of the flow cross-section. The mechanism of hydrate deposition is plotted in Fig. 8, which explains the mechanism of blockage caused by the hydrate growth of the pipe wall film and the regrowth of the hydrate sedimentary layer. Ding et al. [48] also discovered the instability of hydrate sediments, which could cause shedding, regrowth, and redeposition of hydrate deposits. They studied the mechanism of hydrate deposition in water-in-oil emulsions through high-pressure loops, and used the variety of slurry density to characterize the process of hydrate deposition, which was divided into the initial formation of hydrates and deposition stage, the falling off of the hydrate layer deposition from the tube wall, the secondary formation and redeposition, and the deposition aging stage.

Song et al. [49] believed that the implantation and deposition of hydrate particles might be the core of hydrate deposition in oil-based systems. Concerning the clogging mechanism, they held that when the environment met the hydrate formation conditions, the hydrates began to nucleate and grow. Because of the uneven distribution of hydrate particles as well as the continuous increase in particle size and concentration, hydrate particles settled to the bottom and formed an implantation sedimentary layer. With the continuous

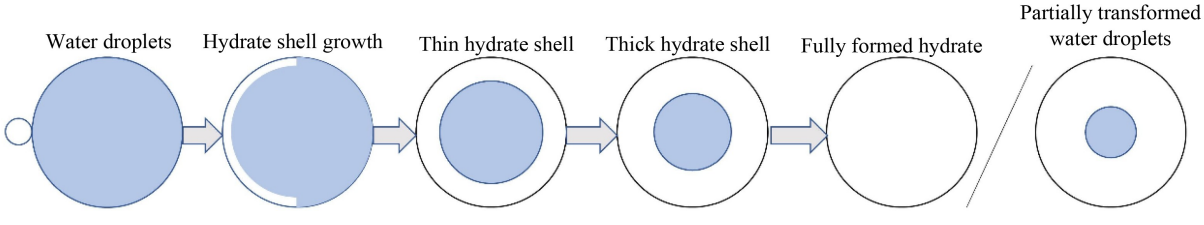

Fig. 7 Inward growth model of hydrate shell (adapted with permission from Ref. [46]).

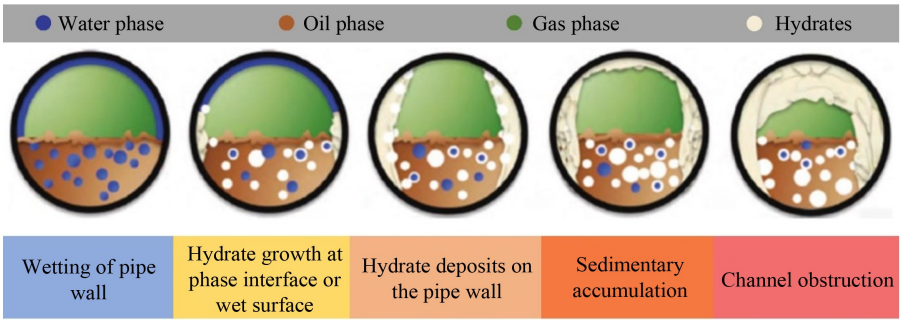

Fig. 8 Conceptual diagram of deposition process of hydrate on pipe wall (adapted with permission from Ref. [47]).

accumulation of the bed, the friction in the pipeline increased and the flow area decreased. Eventually, the bed layer covered the entire flow cross-section and caused local blockage.

In addition, tube wall adhesion of hydrates was also found in the oil-based system, Hu et al. [43] established a kinetic model of oil-based gas hydrate pipe wall adhesion, as manifested in Fig. 9, which shows the effects of interphase drag force F_d (M_d is the additional force couple of the interphase drag force, N·m), the lift force F_l, the adhesion force F_a, and other forces that the hydrate particles receives on the pipe wall. The above-mentioned forces can be roughly divided into the force that promotes attachment of hydrate particles to the pipe wall and the force that promotes the removal of hydrate particles from the pipe wall, according to the effect of the action. The calculation methodology of adhesion can be obtained by Eqs. (4) and (5), and the calculation equation of drag force F_d, additional force couple of interphase drag force M_d and lift force F_l is

$$F_d = 1.7009 \times 6\pi\mu R U_r, \tag{6}$$

$$M_d = 0.944 \times 8\pi\mu R^2 U_r, \tag{7}$$

$$F_l = 6.46\mu R^2 \left(\frac{\rho_l}{\mu} \frac{du}{dy}\Big|_{y=R} \right)^{\frac{1}{2}} U_r, \tag{8}$$

where μ is the viscosity of the liquid phase, Pa·s; U_r is the central velocity of the hydrate particle, m/s; ρ_l is the density of the liquid phase, kg/m^3; u is the liquid phase velocity, m/s. They quantitatively studied the wall adhesion state of hydrates in different environments, and mentioned that the hydrate particles on the tube wall could be removed by rolling (meeting the condition $M_d + F_l l_1 + F_d l_2 > F_a l_1$, and l_1 and l_2 are radial vector.) and pulling up (meeting the condition $F_l > F_a$), and the critical particle size corresponding to the rolling removal method was smaller, which was more likely to occur than stretching relatively.

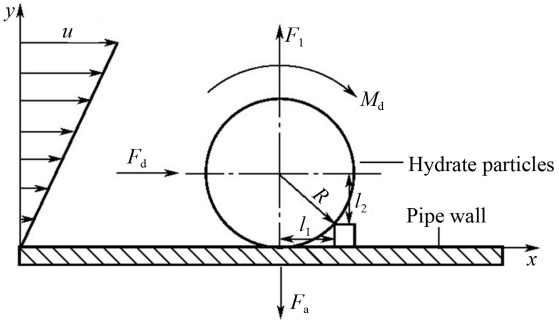

Fig. 9 Force analysis diagram of adhesion of hydrate particles on pipe wall (adapted with permission from Ref. [43]).

In summary, hydrate accumulation, implantation, and wall adhesion may be significant mechanisms for hydrate blockage in oil-based systems. When the tube wall is wet, perhaps the blockage in the oil-based systems are mainly caused by the growth of the tube wall film of hydrate. There are no detailed explanations and distinguishing methods for the diversification of clogging mechanisms in oil-based systems. The authors of the present paper believe that although the oil-water dispersion states in the oil-based system are similar, specific parameters in each study, such as water content, flow rate, particle size, and friction coefficient are obviously different, which lead to different blockage mechanisms. Therefore, the present paper explores the influence of different factors on the risk of hydrate blockage and the mechanism of blockage (described in Section 3.2). The current reports on the flow characteristics of hydrate slurry in oil-based systems have been relatively comprehensive. However, there is still a lack of models related to the process of hydrate accumulation, deposition, and blockage, which can accurately predict the flow of hydrate slurry and the process of pipe blockage under different external conditions and at different flow parameters. Therefore, it is necessary to further model and analyze the clogging mechanisms in oil-based systems under various working conditions, because taking different measures according to different clogging mechanisms is the key to hydrate prevention and control strategies.

3.2 Mechanisms of hydrate blockage in water-based systems

Water-based systems are classified into pure water systems and water-dominant systems. The pure water

systems contains only water or a small amount of gas while the water-dominant systems with water as the main phase contains three phases of oil, gas, and water. Joshi et al. [25] believed that the core of the hydrate blockage mechanism in a high water content system (pure water) was implantation deposition, which was consistent with the results of most scholars. They established a schematic diagram of hydrate blockage mechanism in a high water-cut system. As shown in Fig. 10, the hydrate clogging process in this system includes the following steps: the hydrate particles are uniformly distributed in the initial stage; the system flow is stable; and the pressure drop does not change significantly. With the continuous increase of the number, volume fraction, and particle size of the hydrate, the multiphase fluid in the pipeline gradually changes from a homogeneous flow to a heterogeneous flow, which causes the pressure drop in the pipeline to increase rapidly. $\varphi_{\text{transition}}$ can be used to characterize the hydrate blockage entering a high-risk state, which is defined as the point of sudden increase in pressure drop. Subsequently, the hydrate deposit deposits on the pipe wall. The medium in the system is primarily the gas phase at this moment. The continuous increase in pressure drop and the irregular violent fluctuations can be found, indicating that the hydrate bed layer gradually thickens and becomes unstable. Akhfash et al. [50] used a sapphire autoclave to study the hydrate deposition process, who also observed the transition of hydrate slurry flow from uniform to non-uniform, and eventually forming a sedimentary bed.

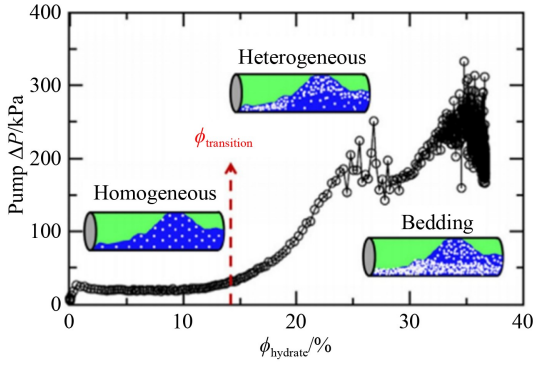

Fig. 10 Schematic diagram of hydrate blockage mechanism in pure water system (adapted with permission from Ref. [25]).

Different from the pure water systems, because the hydrate blockage mechanism of water-dominant systems is more complicated, scholars have numerous different opinions on the research in this area. At present, there are no unified and mature conclusions. Further research is, therefore, urgently needed.

Domestic and foreign scholars have experimentally found that the emulsification state and oil-water dispersion can affect the hydrate deposition in water-dominated systems. Moreover, oil-water demulsification occurs in the system under the action of generated hydrate. Majid et al. [51] observed oil-water demulsification in the process of depositing hydrates in high water-cut systems using high-pressure loops. They found that after the hydrate was formed, the system became the independent continuous oil-water two phase, and hydrates could be formed in the two phases at the same time, based on which, they established a conceptual diagram of oil-water demulsification during the formation of hydrates. As shown in Fig. 11, the higher water content gathers water droplets together and separates them from a thin film. When the hydrate is formed, the surface active components of the oil film are affected, resulting in a decrease in the stability of oil-water emulsion, thereby causing the oil-water phase to separate. In the water-dominated system, the rate of hydrate formation and the total amount of formation are relatively small, and the risk of pipe blockage is low. Because the adhesion force between hydrate particles in the water-dominated system is the van der Waals force with a weaker effect, the adhesion of the pipe wall is unlikely to be the root cause of the blockage in this system. However, the emulsified state and oil-water dispersion degree may be the core of hydrate deposition in the water-dominated system.

The authors of the present paper believe that the oil-water demulsification may be related to the aggregation of particles. The PVM (particle video microscope) image

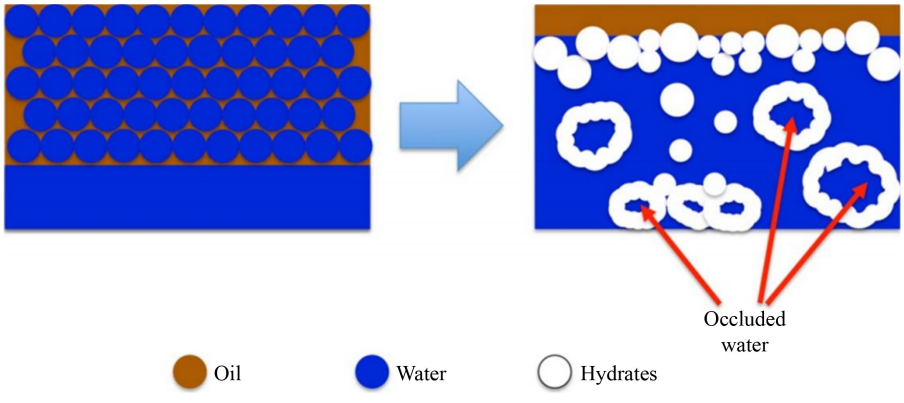

Fig. 11 Conceptual mechanism diagram of oil-water demulsification (adapted with permission from Ref. [51]).

when oil-water demulsification occurs was photographed in Fig. 12. Obviously, there are giant hydrate aggregates in the systems. The oil phase content and the amount of water droplets dispersed in the oil phase are small in high water cut systems. According to the particle aggregation mechanism of Palermo et al., the interaction between the hydrate particles and the water droplets might function in effect as inducing water droplets to form hydrates, thereby consuming the water phase dispersed in the oil phase, which results in the continuity of the oil phase. Few studies have been conducted on the phenomenon of oil-water demulsification. Therefore, research can be administered around this aspect.

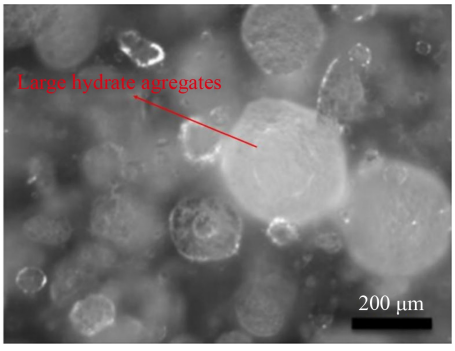

Fig. 12 Oil-water demulsification image taken by PVM (adapted with permission from Ref. [51]).

3.3 Clogging mechanism in PD system

In general, a system with a higher fluid flow rate and a lower water content can form a stable water-in-oil emulsion under the action of flow shear, which is called a completely dispersed system or an oil-based system. When the water content of the system is beyond the phase transition point of water-in-oil emulsion liquid, it is usually considered as a water-based system [52]. When the water content gradually increases, part of the water dispersed in the oil phase in the system separate and exist as free water. This system is referred to as a PD system. Majid et al. [53] used the Mobil loop to explore the hydrate formation and transportation characteristics in PD systems and completely dispersed systems in actual pipelines. They found that the hydrate blockage risk in PD systems were higher than that in completely dispersed systems. At present, most researches are aimed at the hydrate slurry flow in a completely dispersed system, but few studies have been conducted and no unified conclusions have been reached on PD systems. Vijayamohan et al. [54] used the high-pressure loop of the University of Tulsa to study the blockage of hydrates in PD systems and proposed a mechanism. As shown in Fig. 13, the low-viscosity oil in the pipeline carried free water at the bottom flew to the top of the pipe wall to form a water film. After the environment reached the condition of hydrate formation, the water film turned into a hydrate film and blocked the pipeline. Hydrates were conjointly formed on the surface of water droplets or oil-water interface in the oil phase, which consumed tremendous free water to form hydrate mud. Eventually, blockage occurred in the pipeline caused by implantation deposition owing to the increase of friction coefficient and viscosity.

Akhfash et al. [55] studied the hydrate slurry characteristics in PD systems by using a high-pressure transparent reactor, and concluded that the degree of hydrate blockage with a water content of 50% to 70% in a PD system is more severe than that with a water content of less than 30%. They also found that the formation of hydrates in a PD system could cause disturbances at the oil-water interface, which resulted in the fact that the water phase was completely dispersed in the oil phase and accelerated the formation of hydrates. The blockage mechanism diagram of the disturbances of interface is shown in Fig. 14. In a PD system, the initial growth of hydrate particles leads to the destruction of the water-oil

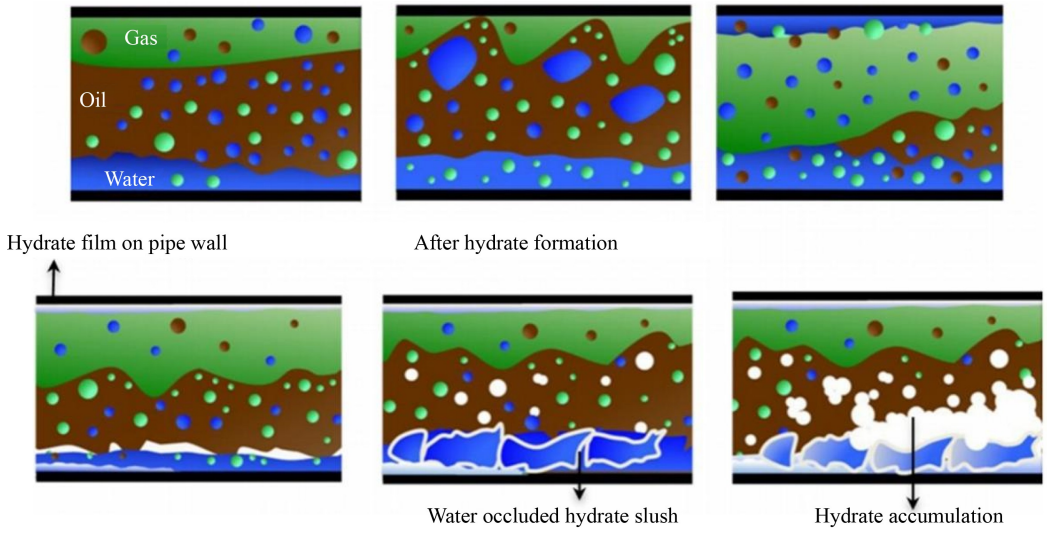

Fig. 13 Growth mechanism of hydrate film in a PD system proposed by Vijayamohan (adapted with permission from Ref. [54]).

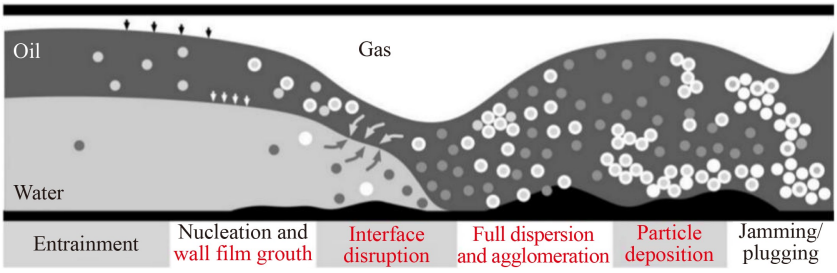

Fig. 14 Schematic diagram of migration of oil-water interface established by Akhfash et al. (adapted with permission from Ref. [55]).

interface, which induces complete dispersion of the water phase in the oil phase and the rapid growth of hydrates. The fully dispersed system may increase the deposition of hydrate particles on the wall, intensifying hydrate blockage.

Grasso [42] proposed that the blockage of the PD system was caused by the hydrate film growth or the wall adhesion of hydrates, which mainly depended on the temperature difference between the fluid and the tube wall and the gas solubility in the bulk phase. Based on the experiment of a self-made rocking reactor, they found that a stronger driving force for film growth prompts hydrates to form on the wall tremendously and quickly when there was a significant difference in temperature, and when the temperature of wall surface was close to that of the fluid, the gas solubility in the body phase replaced the temperature difference and became the main driving force for the formation of hydrates. Hydrates were mainly generated in the bulk phase under the latter circumstance. When the gas solubility was high, the pipe blockage was dominated by the wall adhesion mechanism. A hydrate bed was formed on the bottom of pipe wall and caused pipe blockage when the gas solubility was low.

Taken together, most attention has been directed at the study of oil-based systems, the research on water-based systems, PD systems. The gas-based system has not yet entered the mature stage, and explanations of several microcosms of existing experimental phenomena are not comprehensive enough (such as demulsification caused by the presence of hydrates or migration at the oil-water interface). The liquid water content and flow rate determines the dispersion state of the oil-water two-phase system. Especially, the existence of free water in the PD systems can affect the blocking mechanism. Therefore, quantitative analysis of the free water layer in a PD system is the key to explore the hydrate blockage characteristics of this system. It is worth noting that most of the processes and mechanisms of hydrate blockage, even those widely recognized by most scholars, usually come from assumptions. Current grasp of microscopic evidence about process of hydrate formation republican clogging is far from sufficient. Therefore, it is urgent to study the microscopic state of each phase in the multiphase flow of oil-gas-water in a dynamic system. In addition, a hydrate particle aggregation model and three types of accumulation mechanism models should be established and improved to explore the influence of various factors on hydrate nucleation, growth, aggregation, deposition, and blockage.

4 Factors affecting the blockage under the liquid-rich system in the pipeline

In this section, the effects of flow velocity and water content on hydrate induction time, pipe blocking time, hydrate formation, deposition rate, and pipe blocking mechanism are to be explored in order to provide a theoretical support for the hydrate slurry transportation technology and hydrate blockage prevention and control.

As the direct driving force for the formation of hydrate, temperature and pressure have a significant influence on the blocking tendency in the pipeline. In general, a lower temperature and a higher pressure will lead to a faster rate of hydrate formation, a stronger hydrate film, and a more severe tendency to block the pipe. Several scholars had come to different conclusions about this research. Arjmandi et al. [56] kept the supercooling constant and tested the influence of pressure on the induction period of hydrate formation in systems with and without inhibitors, and found that the induction period did not change significantly, and the induction period was defined as the stage where the system characteristics remained stable before the hydrates crystal nucleation appeared tremendously and grew rapidly. However, scholars had significant differences in the definition of induction time [57]. Generally speaking, the induction period of hydrates can not only measure the ability of the system to maintain a metastable state, but also characterize whether there is a risk of blockage in the mixed transportation pipeline, which is an important kinetic parameter. The authors of the present paper believe that normally, lowering the temperature and increasing the pressure are beneficial to the formation of hydrates and can promote the shortening of the hydrate induction period. In the experiment conducted by Arjmandi, it was discovered that it was possible that the pressure exceeded the limit that can significantly promote the growth of hydrates, which made the pressure factor ineffective. The reason for this might also be that the high concentration of inhibitor added made the effect of pressure promotion not obvious. Further research is needed in this regard.

With the exception of temperature and pressure, there is increasing evidence that the flow rate of hydrate slurry in the pipeline, the water content in the oil-water two-phase system, additives, and other factors have a marked influence on the formation rate, amount of formation, induction time, deposition, and pipe blockage under the liquid-rich system in the flow system [58–62]. Since temperature and pressure are proven to be favorable driving forces for the growth of hydrates, the influence of water content and fluid flow rate on the blockage risk and blockage mechanism in the pipeline have been deeply studied, in order to provide theoretical support for implementation of pipeline blockage risk control and guarantee the security of deep-sea oil and gas flow. Table 2 summarizes some experimental investigations of hydrate slurry flow in the pipeline, hydrate induction period, and hydrate blockage experiments conducted by the domestic and foreign researchers through the various flow experiment loop.

4.1 Effect of fluid flow rate on hydrate blockage

Flow velocity is an external disturbance factor. On the one hand, the larger shearing effect produced by the higher flow velocity leads to smaller water droplets, a larger contact area, and an enhanced mass transfer by reducing the thickness of boundary layer of the interface diffusion. On the other hand, flow system under the enhanced shearing action owing to a relatively high flow rate forms a more uniform emulsion, and the increase in flow rate can make the gas and liquid phase contact more completely which results in improving the degree of mixing and increasing the nucleation sites of hydrates. Therefore, hydrate nucleation is promoted and the induction period is shortened. In addition, the hydrate aggregates or hydrate fixed sedimentary bed in the pipeline would be damaged under the shearing action caused by the high flow rate, and the blockage mechanism of the hydrates would change accordingly, thereby affecting the degree and risk of the hydrate blocking the pipeline. Moreover, the flow rate can also change the viscosity and friction coefficient of the hydrate slurry and make it shear thin [70–72].

Shi et al. [73] studied the flow characteristics of the hydrate slurry in the water-in-oil emulsion system and found that with the increase of the flow rate, the friction coefficient of the system decreased significantly. They believed that there was a critical suspension height in the

Table 2 Summary of the investigation of the loop experimental of hydrate

Ref.	Time	Experimental device or method	Hydrate guest molecule type	Main research content	Research result
[63]	1995	High-pressure wheel loop	Methane, ethane, propane hydrate	Inhibition performance of chemical additives on gas hydrate	Most kinetic inhibitors can increase the degree of supercooling required for the formation of hydrates, thereby inhibiting the formation of hydrates
[64]	1999	NTNU (Norwegian University of Science and Technology) loop experiment	Methane or a mixture of methane, ethane, and propane	Flow characteristics of hydrate slurry under different hydrate concentrations	The apparent viscosity of the hydrate slurry increased with the increase of the hydrate concentration; in the turbulent state, the frictional pressure drop of the hydrate slurry was only determined by the nature of the water-carrying phase
[33]	2002	Archimede Loop	Methane hydrate	Influence of dispersant and kinetic inhibitor (PVP) on the formation and fluidity of methane hydrate slurry	The concentration of additives had a significant impact on the flow characteristics of water-in-oil emulsions and hydrate slurries, and additives can effectively alleviate pipe blockage
[65]	2012	ExxonMobil loop	He, N_2, CO_2, etc.	Main factors affecting the formation of hydrate slurry	Determination of the main parameters affected the transportation of hydrate slurry
[25]	2013	ExxonMobil loop	CH_4	Mechanism of hydrate formation and blocking in the high water content system	The mechanism was the increase of interaction and agglomeration between particles, which ultimately led to the formation of hydrate beds and wall deposits
[66]	2014	Small flow loop experiment	CH_4+C_3H_8/CH_4+i−C_4H_{10} two-component gas hydrate	Effect of dual kinetic inhibition of PVP and L-Tyrosine on the induction period of binary component gas hydrate formation	The simultaneous addition of PVP and L-Tyrosine increased the induction time of gas hydrate formation several times, which was more effective than adding PVP alone as a kinetic inhibitor
[58]	2014	High-pressure hydrate experimental circuit	Natural gas hydrate	Influence of subcooling, supersaturation, flow rate, water content, and polymerization inhibitor concentration on the induction period of natural gas hydrate formation	Induction time was inversely proportional to the degree of subcooling; as flow rate and supersaturation increase, the induction time presented a V-shaped curve or gradually increased; the induction time decreased first and then increased with the increase of water content
[67]	2014	IFP-Lyre (Institut Francais Du Petrole) loop experiment	CH_4	Influence of factors such as moisture content, liquid phase flow rate, and polymerization inhibitors on the flow characteristics of hydrate slurry in the case of high water content	The higher the water content, the more difficult it was to crystallize the hydrate; addition of AA-LDHI (Anti-Agglomerates and Low Dosage Hydrate Inhibitor) could effectively maintain the fluidity of the pipeline
[68]	2014	University of Tulsa loop	Natural gas hydrate	Mechanism of hydrate formation and blocking in the PD system	The growth of hydrate/sediment on the tube wall seemed to be the dominant phenomenon of hydrate growth in PD systems
[69]	2017	CUPB (China University of Petroleum, Beijing) storage and transportation experimental loop	Natural gas hydrate	Mechanism of hydrate formation and blockage under different gas-liquid flow patterns	The blocking mechanism and pipe blocking tendency of hydrates were different under different flow patterns. (mentioned later)

pipeline which balanced the lift force on the hydrate generated by the velocity gradient with the gravity of the particles. The velocity gradient increased as the distance between the particles and the pipe wall decreased. Thereby, the higher velocity, the farther critical suspension height was from the pipe wall. When the critical height was about 71% of the entire pipeline, the friction caused by the interaction between the hydrate and the pipe wall could be ignored and would not be affected by the suspension height. In this stage, the particle flow was relatively stable. Therefore, the particles could be suspended in this area by controlling the flow rate of the actual operating pipeline, which might effectively maintain the safe transportation of the pipeline.

Liu et al. [35] studied the flow characteristics of hydrate slurry at different liquid loads and mixing speeds based on a fully visualized flow circuit. They divided the flow of hydrate slurry under multiphase flow conditions into hydrate formation (stage I), aggregation (stage II), sedimentation (stage III), and implantation (stage IV) according to the variety in the flow rate of the mixture and pressure drop. The hydrate formation volume fraction at different flow rates, the mixture flow rate, the pressure drop, and the temperature change are shown in Fig. 15. Obviously, the hydrate formation rate in the first three stages at a high flow rate is higher than that at a low flow rate, and in the third stage at a high flow rate lasts longer. This means that increasing the flow rate can increase the rate of hydrate formation. In addition, the transition time from deposition to implantation at a high flow rate is longer than that at a low flow rate. The reason for this is that the influence of the mixture flow rate on the critical implantation rate, which causes hydrate implantation deposition at a high flow rate is inhibited [74, 75]. However, the report did not explain the weakened sedimentation. Figure 16 shows the effective hydrate volume fraction and water conversion rate at different flow rates (Cases 2 and 3). The increase in the mixture velocity means frequent gas-water contact, which leads to a higher hydrate volume fraction and water conversion rate. In the initial stage, the lower flow rate has a higher water conversion rate. The reason for this might be that, in this stage, the low flow rate generates less frictional heat, which would not affect the heat transfer in the water conversion process. Subsequently, the mass transfer of gas to water caused by high flow rate is dominant, so that the water conversion rate increases with the increase in flow rate.

The authors of the present paper believe that although Liu et al. comprehensively introduce all the parameters and macro characteristics of each scheme, there are few experimental programs and only two sets of experimental controls for one factor, whose conclusion is yet to be verified. In addition, Liu's experiment does not mention the effect of flow rate on the aggregation of hydrate particles, and there are no microscopic image and specific description of the interaction between hydrate particles during the hydrate aggregation stage. Blockage of hydrates is a comprehensive and complex process, micro and macro phenomena and parameter changes should be combined to understand the behavioral characteristics of hydrates. An in-depth analysis of the hydrate deposition and aggregation process may provide a more comprehensive understanding of the flow behavior characteristics of hydrate slurry.

Regarding the effect of flow velocity on hydrate deposition and implantation, Ding et al. [48] had different conclusions. As shown in Fig. 17, they studied the

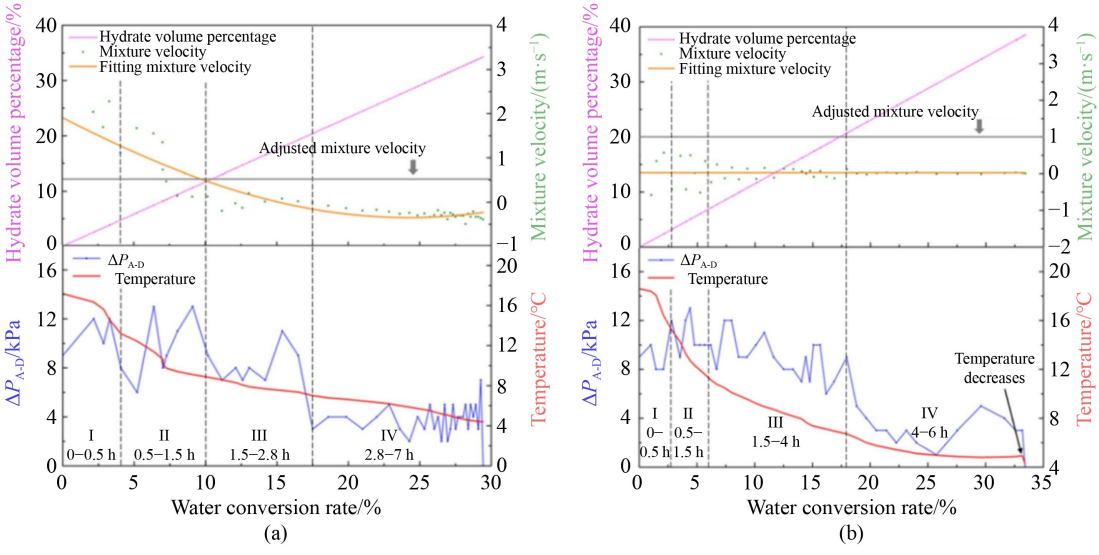

Fig. 15 Variation of hydrate formation volume fraction, mixture flow rate, pressure drop, and temperature at different flow rates (adapted with permission from Ref. [35]).

(a) At a low flow rate; (b) at a high flow rate.

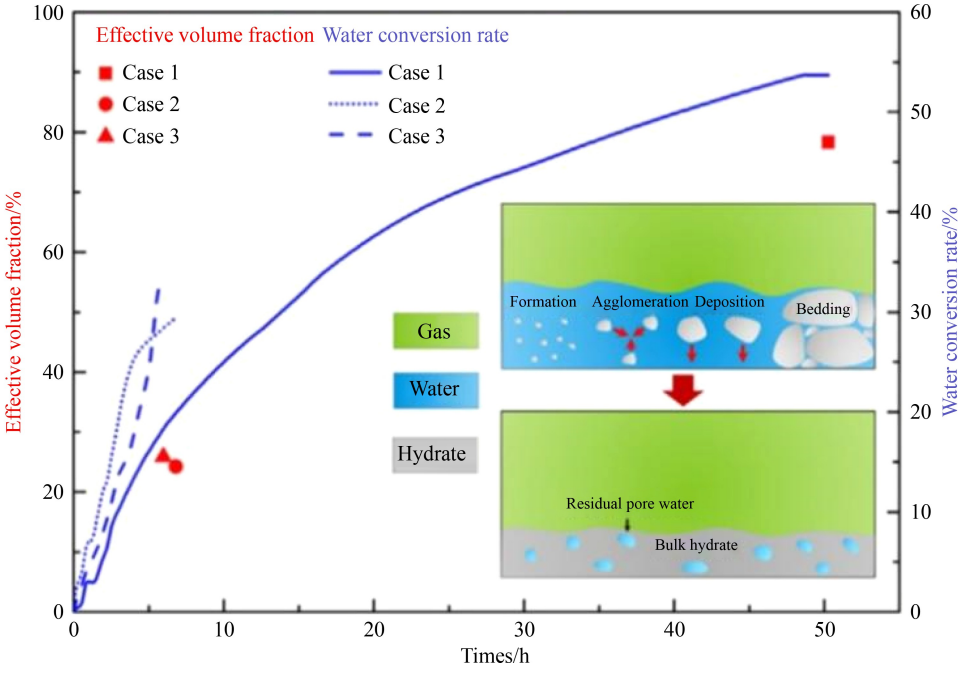

Fig. 16 Schematic diagram of effective volume fraction and water rate conversion in different flow rate systems (adapted with permission from Ref. [35]).

deposition rate and deposition thickness at five different flow velocities in the same water content and dosage of anti-aggregation agent and found that the hydrate deposition rate and deposition thickness both increased first and then decreased and the maximum value occurred at a flow rate of 1650 kg/h. This experimental phenomenon can be explained as follows. According to the conclusion of Rao et al. [76], hydrate deposition can be understood as the mass transfer process between the liquid body and the pipe wall surface. This process should be related to the mass transfer coefficient of the tube wall surface, which can be characterized by the Sherwood number.

$$Sh_{\mathrm{D}} = 0.023 Re_{\mathrm{D}}^{\frac{4}{5}} Sc^{\frac{1}{3}}, \tag{9}$$

where Sh_{D} is the Sherwood number, Re_{D} is the Reynolds number, and Sc is the Schmidt number. For a particular system, a higher flow rate resulted in a larger Reynolds number which results in a larger Sherwood number. Accordingly, a higher flow velocity can enhance the hydrate deposition process by enhancing the mass transfer coefficient on the pipe wall surface. Therefore, when the flow rate increases from 600 to 1650 kg/h, the hydrate deposition rate increases. However, a further increase in the flow rate can increase the flow shear rate on the pipe wall surface. The strong flow shear rate makes it difficult for the hydrate particles to adhere to the pipe wall, and even causes the sediment layer to fall off. These characteristics dominate the changes in deposition rate and deposition layer thickness.

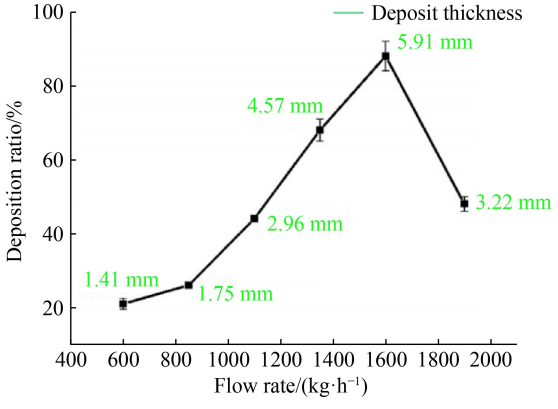

Fig. 17 Variation in hydrate deposition rate and deposition thickness at different flow rates (adapted with permission from Ref. [48]).

The fluid velocity had a significant effect on the rate and quantity of hydrate formation [77], the variation in fluid velocity and the formation of hydrate could affect the flow patterns, which also had a marked influence on the hydrate blockage mechanism [69]. Based on the method of characterizing the aggregation and deposition characteristics of hydrates by particle density variations and chord length distributions, Ding et al. [78] analyzed the mechanism of hydrate blockage under different flow pattern conditions. The flow pattern was modified by changing the gas-liquid flow rate and relied on the visual loop to determine. Figure 18 shows the change of the parameters of each flow pattern versus time. Several macro features at the viewing window are shown in Fig. 20.

Under all flow conditions, the relative pressure drop (the ratio of pressure drop to flow rate) increases in the stage of hydrates formation. As shown in Fig. 18(a),

when the hydrates in the stratified flow begins to form at about 1.7 h, the whole number of hydrate particles/droplets decreases rapidly, indicating that hydrate agglomeration has occurred at this time. Subsequently, hydrate formation leads to an increase in the number of particles. The variation of mud density is not prominent after the hydrate is formed, indicating that the degree of hydrate deposition in the stratified flow is slight. In addition, the total number of hydrate particles in the liquid phase continues increasing after the initial stage, which also means that hydrate particles tend to grow in the liquid phase instead of depositing on the surface of the tube wall. Therefore, the blockage in the stratified flow is dominated by the continuous growth and accumulation of hydrates in the liquid phase. According to the image and analysis, the blockage mechanism of the stratified flow is shown in Fig. 19(a), where (i) indicates the dispersion of water droplets in the oil phase; (ii) the hydrate nucleation; (iii) the beginning of aggregation of hydrate particles and water droplets with each other; (iv) the aggregates growth; (v) the deposition of aggregates on the pipe wall and blocked the pipe.

The reason for the formation of bubbly flow is that the system flows in a very small gas flow rate and its parameter changes are similar to the stratified flow. As shown in Fig. 18(b), in this flow pattern, the aggregation of particles also occur after the formation of hydrate. It is worth noting that the total number of particles starts to increase after the formation of hydrates because of the continuous formation of hydrates rather than bubble bursting and aggregate decomposition, which can be proved by the increase in the average chord length of the particles. Then, the total number of particles and slurry density begins to decrease, which makes the authors infer that this is caused by the hydrates deposited on surface of pipe wall. In the end, a stable state is maintained in the system and no blockages are formed. The blockage mechanism of the bubble flow is shown in Fig. 19(b), where (i) indicates the dispersion of water droplets in the bubble flow in the oil phase; (ii) the formation of hydrates at the water/oil interface; (iii) the aggregation of hydrate particles and water droplets with each other; (iv) the growth of aggregates; and (v) the deposition of hydrates and agglomerates on the surface of the pipe wall, and the maintaining of the system in a stable flow state.

In the slug flow, the decrease in the density of slurry when the hydrates begin to form indicates that the deposition and accumulation of hydrate occur at an equivalent time. As shown in Fig. 18(c), the massive flow fluctuation of the slug flow increases the frequency of contact between the hydrate particles and the pipe. The

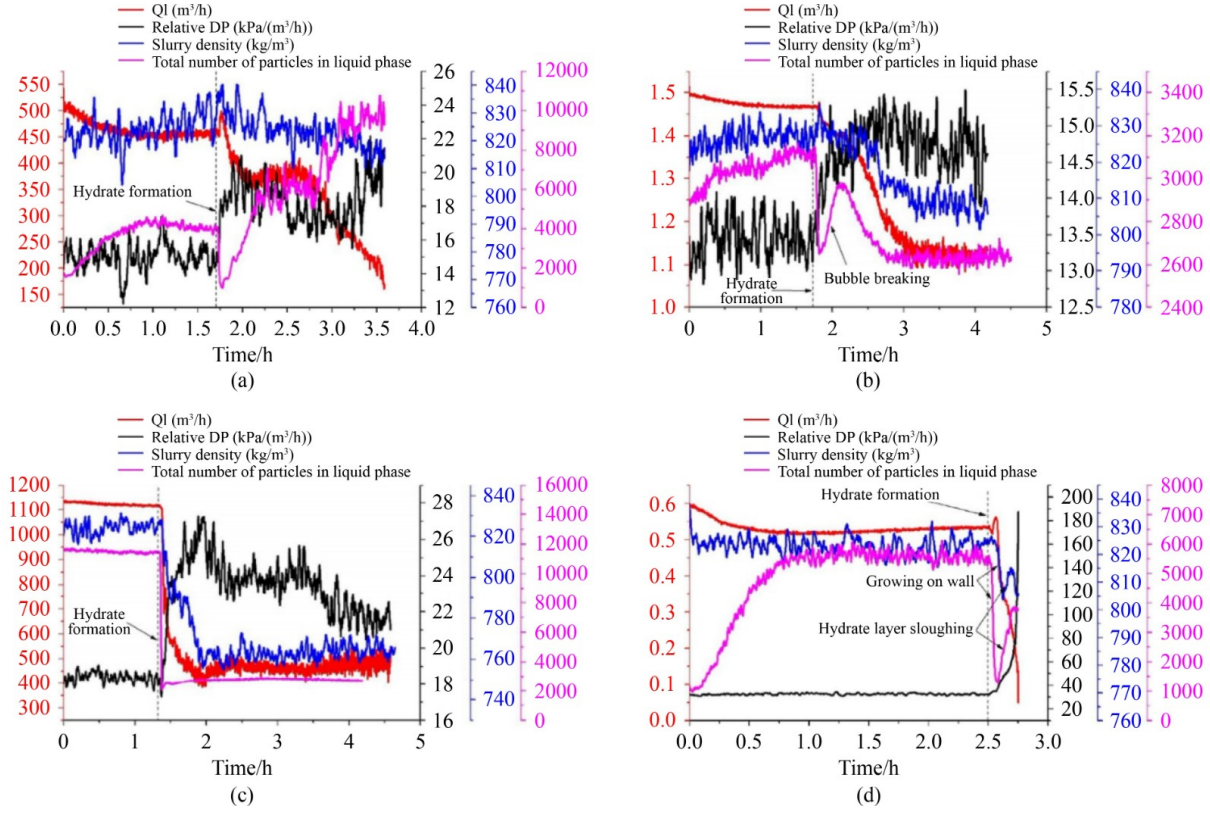

Fig. 18 Change of flow rate, relative pressure drop, slurry density, and the number of particles in the liquid phase in different flow patterns (adapted with permission from Ref. [78]).

(a) Stratified flow; (b) bubble flow; (c) slug flow; (d) annular flow.

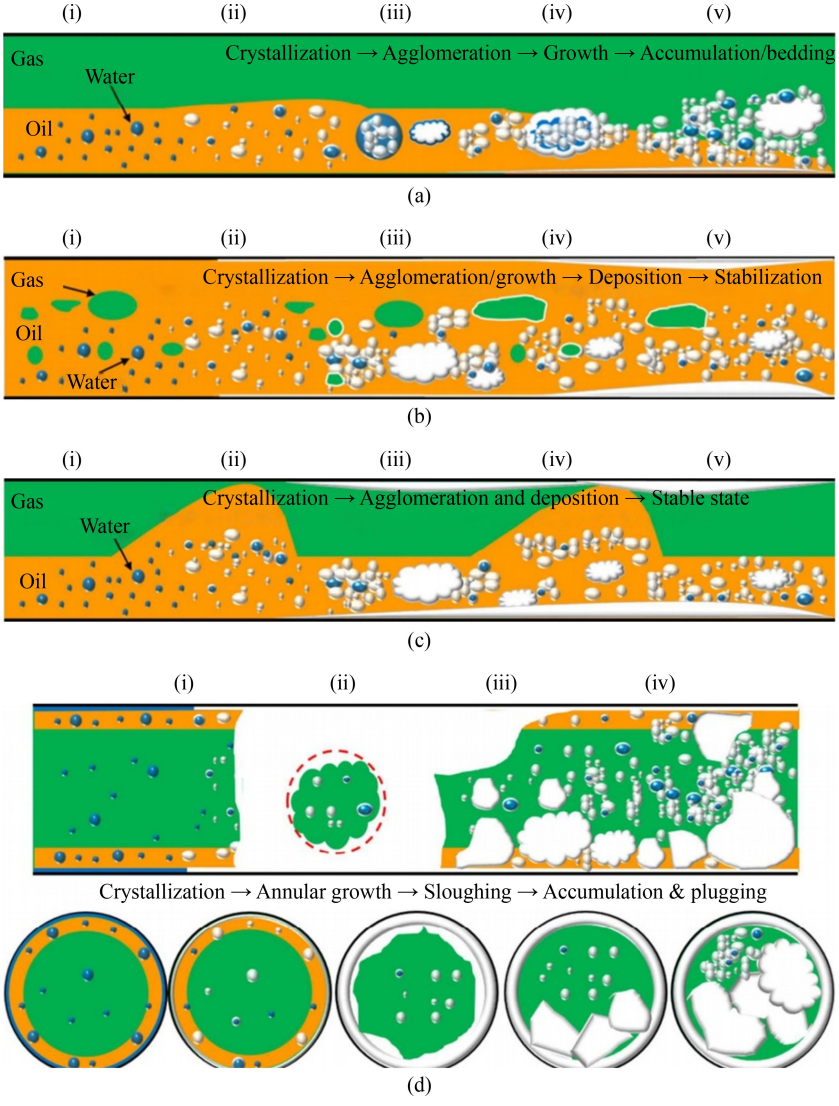

Fig. 19 Schematic diagram of hydrate blockage mechanism under different flow patterns (adapted with permission from Ref. [78]). (a) Stratified flow; (b) bubbly flow; (c) slug flow; (d) annular flow.

deposition process in slug flow occurs earlier than other flow patterns. Then, the smooth variation of slurry density indicates that the deposition process stops. According to measurements, during this period, the average chord length decreases slightly and the total number of particles increases slightly, which indicate that some hydrate agglomerates are decomposed. But this phenomenon is accidental and might not be regarded as a typical feature of slug flow. Then, the system remains stable and does not form a blockage. The mechanism of slug flow is shown in Fig. 19(c), where (i) indicates the dispersion of the water droplets in the slug flow in the oil phase; (ii) the beginning of nucleation of hydrates at the water/oil interface; (iii) the condensation of hydrates and water droplets in the liquid phase or deposition on the surface of the pipe wall at the same time; (iv) the decomposition of some agglomerates by the shear force of the fluid (may not happen); (v) the maintaining of the system at a stable flow state.

The macroscopic phenomenon of the annular flow is shown in Figs. 20(c) and 20(d). The immediate reduction in the density of slurry and the number of particles is caused by the fact that the hydrate directly forms a hydrate layer on the pipe wall. Then the density of the slurry and the number of particles begin to increase. At an equivalent time, the hydrate layer formed begins to fall off and the circuit is immediately blocked. As shown in Fig. 18(d), it is inferred that the blockage is caused by the fact that shedding hydrate fragments aggregate and get stuck somewhere in the loop. The blockage mechanism of the annular flow is shown in Fig. 19(d), where (i) indicates the dispersion of water droplets in the annular flow in the oil phase or their distribution in the form of a water film covering the pipe wall; (ii) the beginning of

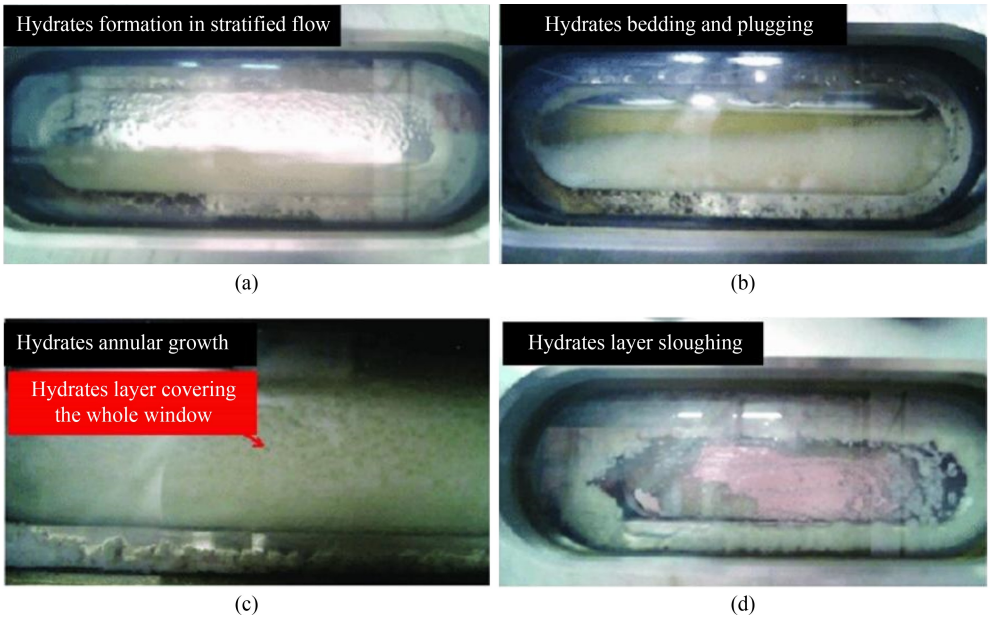

Fig. 20 Behavior characteristics of hydrate slurry in specific flow patterns (adapted with permission from Ref. [78]).
(a) Hydrates formation in stratified flow; (b) hydrates bedding and plugging; (c) hydrates annular growth; (d) hydrates layer sloughing.

the formation of hydrates on the pipe wall or the oil-water interface, forming a thick hydrate layer covering the pipe wall; (iii) the beginning of the falling off of the hydrate layer due to shearing force; (iv) the gathering of the fallen hydrate fragments somewhere in the pipeline and blocking of the flow cross section.

However, it should be noted that in the experiment of Ding et al., the flow patterns were controlled by changing the gas-liquid flow rate, and the water content in the system was constant. Hydrate plugging was a complicated process which could be affected by many parameters. Therefore, if the influence of water content was not considered and only the influence of flow rate was analyzed, the blocking mechanism of each flow pattern could not be proved under different water content conditions. It is necessary to fully consider the influence of various factors. In addition, Ding et al. determined the flow characteristics of hydrate slurry, such as deposition and aggregation, based on changes in parameters such as density, liquid phase particle number, and particle size chord length. However, there were no supports of microscopic phenomenon for each state of hydrate to prove their conjectures. Thereby, scholars can consider using some microscopic devices, such as focused beam reflectance measurement, to combine specific microscopic phenomena and parameter changes to analyze the flow characteristics of slurry.

In summary, from the aspect of hydrate nucleation, increasing the flow rate would promote the mass transfer between phases and increase the possibility of hydrate nucleation, and result in a shortened hydrate induction period and an increase in the amount and rate of hydrate formation. In addition, based on the hydrates blockage mechanism of oil-based systems, increasing the flow rate can not only destroy the hydrate polymer formed, but also increase the effect of the flow shear force on the hydrate particles which reduces the probability of adhesion between the particles. At a high flow rate, the tendency of hydrate to deposit on the pipe wall is small and the stability of the deposit layer is poor. The rheological properties of hydrate slurry accord with shear thinning, which means that increasing the flow rate can reduce the viscosity of the system and keep it in a stable flow state. Under the dominance of these factors, the risk of pipe blockage is significantly reduced. Therefore, considering the two aspects of hydrate nucleation and blockage mechanisms, the authors of the present paper believe that there might be a flow rate threshold. When the flow rate is lower than this threshold, the risk of hydrate blockage increases with the increase of the flow rate, and increasing the flow rate can relieve the blockage when the flow rate is higher than this threshold. Therefore, it is possible to model the blockage of pipelines at different flow rates and in flow patterns to explore the quantitative analysis of flow factors on the blockage, which may lead to some novel conclusions regarding the effect of flow velocity on the blockage.

4.2 Influence of water content on blockage of hydrate

The flow rate factor is complex, so is the water content. Water content is the key parameter of the oil-water emulsification system. According to the difference in water content between different systems, the system can be divided into Water-based, oil-based, and PD systems. The mechanism and risk of clogging in the system at different water contents must be different. Akhfash et al.

[55] of the University of Western Australia used mineral oil in a water content of 10%–70% as a medium to study the clogging mechanism of hydrates in a PD system and found that when the water content was below 30%, the degree of blockage would not change significantly due to the variation of water content. However, the degree of hydrate blockage would become more severe as the water content increases to 50%–70%. The degree of blockage of the pipeline by hydrate is greatly improved compared with that in the low water content. The water content would have a significant effect on the flow parameters, friction coefficient, pressure drop, fluid flow patterns, and viscosity of the hydrate slurry. Therefore, the ability to control the water content in the oil-water two-phase system to alleviate the tendency of pipe blockage in the system is particularly important for the safe transportation of pipelines.

Lv et al. [18], using CO_2, deionized water, and industrial white oil as the experimental medium, explored flow rate (25–35 kg/min), carrier liquid volume (7–9 L), water content (60%–100%), and initial pressure (2.5–3 MPa) on the induction time of hydrate formation based on the high-pressure flow loop. According to the linear regression coefficient method, the sensitivity of each factor was ranked. They found that water content had the most significant influence on hydrate induction time. In addition, after comparing the hydrate formation and slurry flow characteristics in pure water systems and oil-water emulsion systems, they found that the pressure drop and apparent viscosity in oil-water emulsion systems were far higher than those in pure water systems, which indicated that the emulsion system was more prone to blockage. As the water content increased, the induction time required for the formation of hydrates in oil-water emulsion systems was gradually shortened. They believed that increasing the water content would reduce the number of oil droplets dispersed in the water phase, which weakened the influence of oil droplets on bubbles and increased the chance of combination of gas and water. In addition, the decrease in the number of oil droplets around the generated crystal grains increased the growth rate of hydrate crystals. Therefore, with the increase in the water content, th macroscopical induction time was shortened and the final volume fraction of hydrate at the end of the experiment increased. The result of induction time and hydrate volume fraction is shown in Fig. 22. Therefore, the average friction coefficient and average apparent viscosity in the stable phase were also increased with water content owing to tremendous formation of hydrate. The average friction coefficient and average apparent viscosity are shown in Fig. 23. This conclusion was the same as the effect of water content on viscosity measured by Ding et al. [79].

The authors of the present paper speculate that the increase in water content not only enlarged the formation of hydrate, but also intensified the aggregation of hydrate particles. The combined effect of the two led to the increase in the average friction coefficient and average apparent viscosity. This can be combined with images taken by the microscopic experimental device for in-depth research.

It should be noted that in the 80% water content system, the experiment on the influence of water content on the final volume fraction of hydrate was insufficient

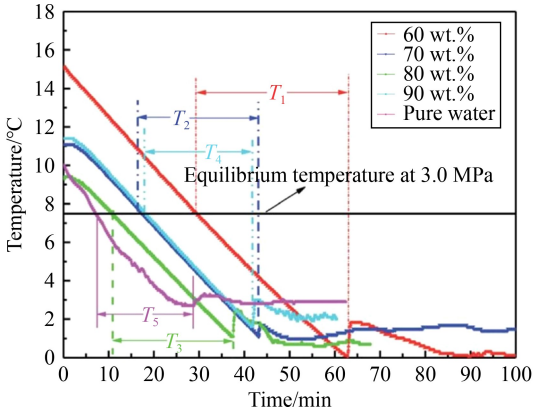

Fig. 21 Temperature-time curves at different water contents during formation of hydrates (adapted with permission from Ref. [18]).

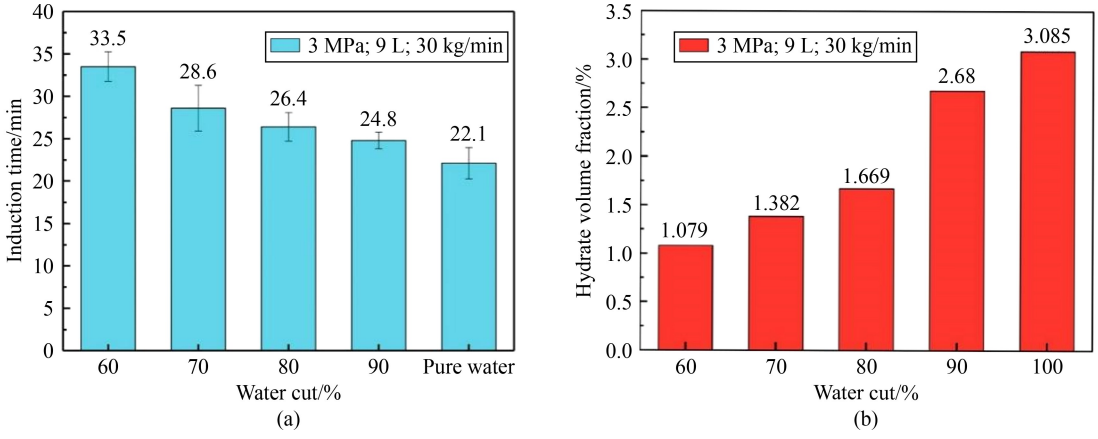

Fig. 22 (a) Hydrate induction time and (b) hydrate volume fraction at different water contents (adapted with permission from Ref. [18]).

because of occurrence of pipe blockage, because the shearing effect of fluid flow always acts on the hydrate nucleation process before the pipeline is blocked by the hydrate. Hydrate formation process might not finish spontaneously after the pipeline is blocked, but is forced to stop owing to changes in external disturbance factors. Therefore, if the final hydrate value measured is the amount of hydrate generated when the pipe is blocked, i.e., when the flow is zero, it is impossible to clearly characterize the true amount of hydrate generated in the flowing system, which would bias the experimental results.

What is interesting is that there are different experimental results about the effect of water content on hydrate induction time. Lv et al. [58] experimentlly studied hydrate induction time under the conditions of adding 1%, 2%, and 3% of anti-polymerization agent and found that the induction time first decreased and then increased as the water content of the system increased. This was in stark contrast to the result of induction time which was inversely proportional to water content. The authors of the present paper believe that the reason for this may be that on the one hand, a higher water content produces a larger gas-water interface area, which leads to more nucleation sites and accelerated formation rate of nucleation; on the other hand, the increase in water content would also lead to the decrease of gas solubility in unit volume of oil-water emulsion during nucleation and growth, which limits the mass transfer of the gas and reduces the nucleation and growth rate of hydrates.

The water content would also affect the hydrate deposition rate and the thickness of the sedimentary layer. Ding et al. [48] explored the influence of four different water contents in systems with two different flow rates on hydrate deposition at the same content of anti-polymerization agent. The results were shown in Fig. 24. Obviously, for water-in-oil emulsion systems, both the deposition rate and thickness of hydrate were directly proportional to the water content in the systems. As the water content increased, the more severe the hydrate deposition became. The reason for this is that the amount of hydrate formation in a high water cut system is more tremendous, which is in good agreement with the explanation of Lv et al. In addition, the amount of adhesion water in a high water content system is also larger, resulting in a larger hydrate deposition rate. Accordingly, with the increase of water content, the amount of hydrate deposition increased significantly attributable to the higher amount of hydrate formation and adhesion water.

Additionally, the difference in water content also affected the flow characteristics, the morphological evolution of the hydrate in the pipeline, the pipeline blockage process, and the blockage mechanism. Song et al. [49] conducted a hydrate blockage experiment under different water content and flow rate conditions and found that the free continuous water phase existing in the high water content system could adhere to the wall surface in the form of splash, causing the hydrates to simultaneously form on the main body of the liquid phase and the wall of the pipe. The higher water content reduced the mass fraction of hydrates and shortened the blocking time, making it impossible for the hydrates in the pipeline to form a stable sedimentary layer. In addition, when the friction increases and the flow rate decreases, the weakening of shearing effect cause the oil and water to stratify under the action of gravity owing to the abundant free water phase.

In the low water content system, most or all of the water phase were dispersed in the oil phase and the hydrates were only formed in the main body of the liquid phase in the form of fine sand. The hydrate sedimentary layer formed was in the form of flocs. The lower water content caused the free water in the system to be exhausted due to the formation of hydrate. Therefore, there was no oil-water stratification phenomenon. The morphology of the hydrate slurry in the two systems was

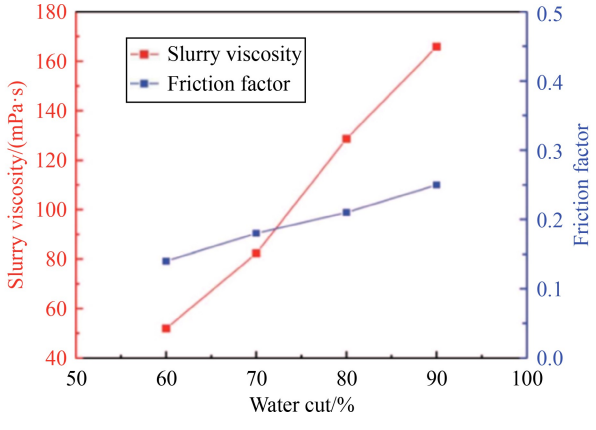

Fig. 23 Apparent viscosity and friction coefficient of hydrate under different water contents (adapted with permission from Ref. [18]).

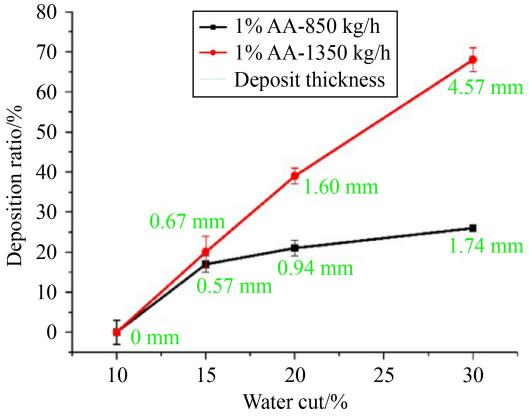

Fig. 24 Deposition rate and thickness of hydrate at different water contents (adapted with permission from Ref. [48]).

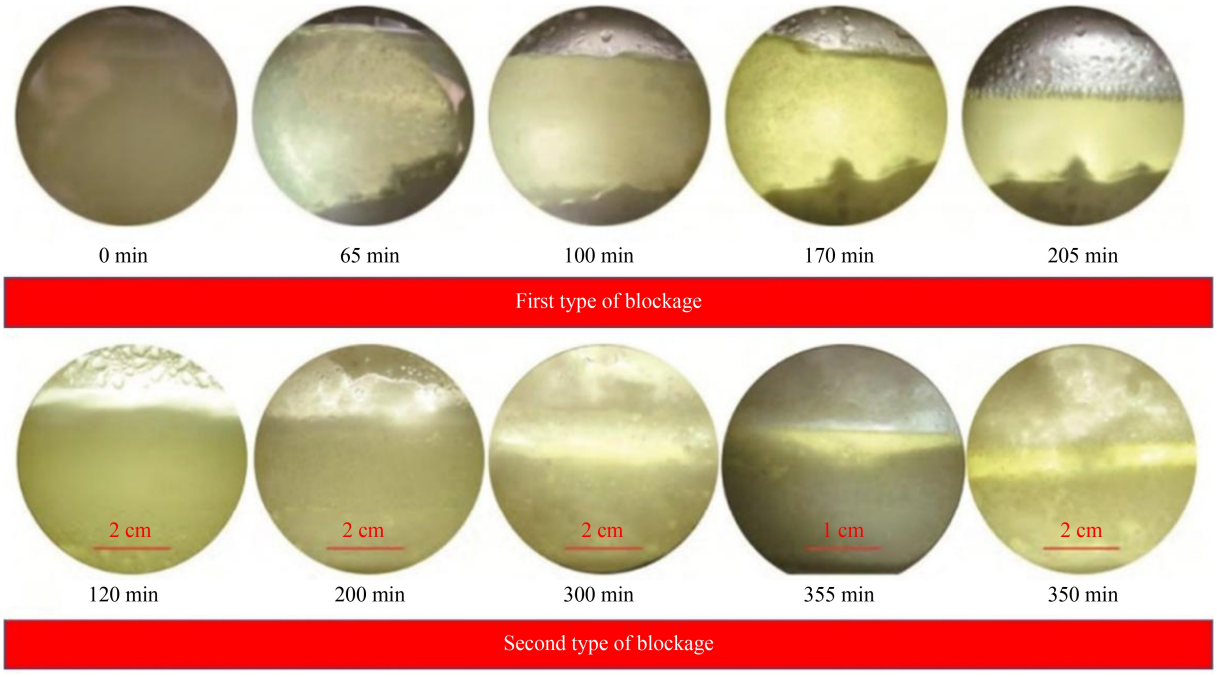

Fig. 25 Formation of hydrates in pipeline during two types of blockage processes (adapted with permission from Ref. [49]).

shown in Fig. 25. Song et al. proposed two clogging mechanisms based on the difference in water content. The clogging mechanism of the first type (in a low water content system) was that the continuous growth of hydrates made the hydrate concentration in the system continue to increase. Consequently, the formation of hydrate deposits was observed at the bottom of the pipeline. The deposited layer underwent secondary growth and thickening, which increased the friction in the system and eventually blocked the pipeline. The clogging mechanism of the second type (in a high water content system) was that, with the increase in the friction and the decrease in the flow rate, the oil and water phases that were originally evenly distributed in the pipeline would be stratified due to gravity. The concentration of the slurry mixture on the bottom in the liquid phase caused the fluid viscosity to dramatically increase. When the viscosity and frictional resistance of the system reached a certain level, the fluid would completely lose its fluidity and result in blockage eventually. The mechanism of the two types of pipe blockage is shown in Fig. 26.

In summary, the water content in an oil-water two-phase system not only affected the hydrate growth and hydrate induction time, but also affected the oil-water two-phase dispersion in a liquid-rich system. The variation of the oil-water dispersion state could lead to a change in the morphology of hydrate formation and clogging mechanism. In general, the risk of pipe blockage in a PD system was higher than that in a fully dispersed system. Additionally, the water content would change the basic phase in the liquid-rich system, which also affected the flow behavior of the hydrate slurry and the blocking mechanism. Eventually, the influence of the free water layer in PD systems on the plugging mechanism and the diversity of the plugging mechanism in the oil-based system owing to different water content are still in the research stage, which need to be studied in-depth.

5 Model of hydrate in rich liquid system

The formation of hydrates in the pipeline is the result of the combined effects of intrinsic kinetics, heat transfer, and mass transfer [80]. Accumulation, deposition, bedding, and blockage of hydrate in the pipeline are not only related to thermodynamic driving force, intrinsic kinetics, and mass transfer limitation, but also the function of flow velocity, water content, gas-liquid ratio and physical and chemical parameters of gas and liquid phases, etc. [81]. At present, relevant models for hydrate formation, adhesion, deposition, and accumulation have been reported [13, 82–84]. Through the in-depth understanding of the mechanism behind the hydrate flow behavior through various models, it is possible that the solution of hydrate risk management through prediction technology as the technical guidance for a new type of hydrate treatment will be better than the traditional hydrate blockage prevention and control strategy. Therefore, it is imperative to establish a comprehensive model of hydrate blockage in gas-liquid-solid pipelines. The present paper mainly summarizes the various related behaviors of the formed hydrate in the form of slurry in the flow state and the modeling of the clogging tendency.

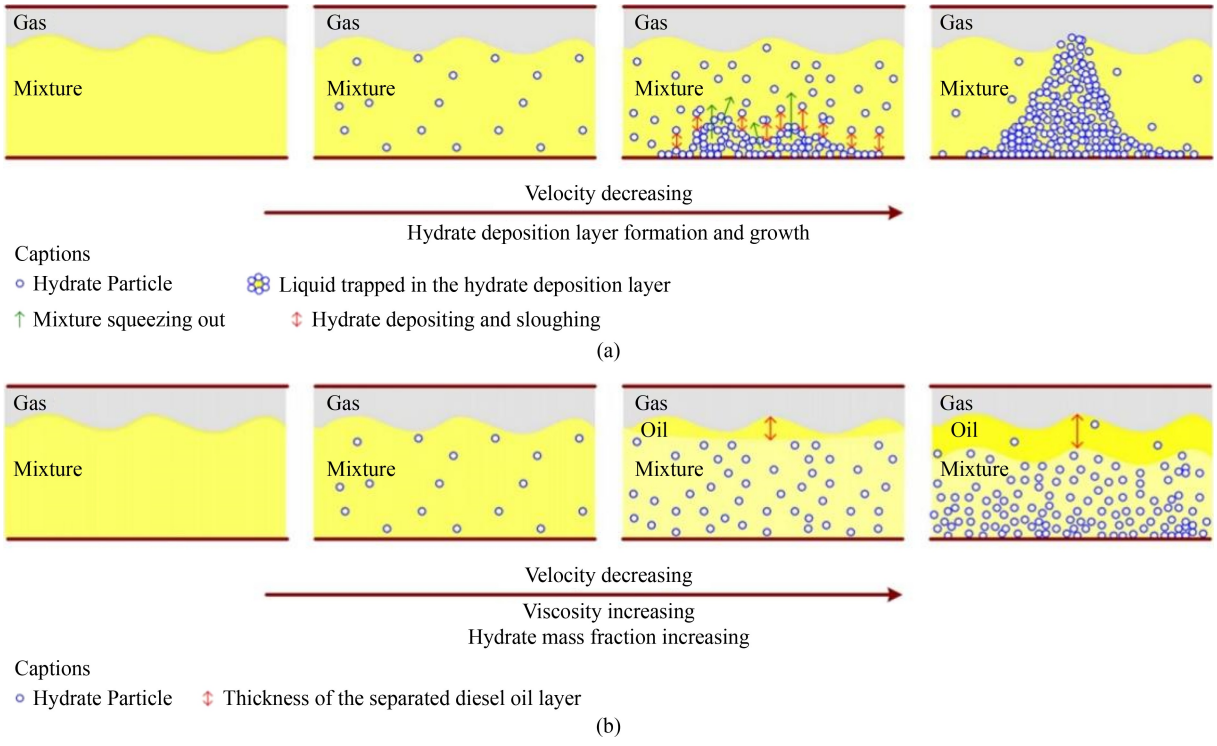

Fig. 26 Schematic diagrams of mechanisms of two types of blocking processes (adapted with permission from Ref. [49]). (a) The first category; (b) the second category.

5.1 Hydrate bedding model

Based on the energy required to balance the suspended solids and the energy dissipated by the turbulent eddies in the two-phase solid-liquid turbulence, Oroskar et al. [85] proposed the steady-state correlation of the critical velocity of the hydrate slurry flow in the oil-based system. Correlation was applicable to multiphase flow systems with interaction between hydrate particles. Applying this correlation to hydrate slurry transportation, the critical velocity of bedding (v_c) was calculated as

$$v_c = 1.85\varphi_l^{0.1536}(1-\varphi_l)^{0.3564}\left(\frac{d_A}{D_p}\right)^{-0.378}\bar{N}_{Re}^{0.09}\sqrt{gd_A(s-1)}, \tag{10}$$

$$\bar{N}_{Re} = [D_p\rho_{oil}\sqrt{gd_A(s-1)}/\mu_{oil}, \tag{11}$$

where d_A are the sizes of the hydrate agglomerates, φ_l is the volume fraction of the hydrate (relative to the liquid phase), μ_{oil} is the viscosity of the oil phase, g is the acceleration of gravity, s is the ratio of hydrate density to oil phase density (ρ_{hyd}/ρ_{oil}), D_p is the inner diameter of the pipe, and $\bar{N}_{Re}$ is the modified Reynolds number, defined in Eq. (11). The critical hydrate aggregate size that can exist under the flow shear force corresponding to the critical liquid suspension velocity can be calculated by

$$d_{A,crit}^{0.167} = \frac{v_c}{1.85\varphi_l^{0.1536}(1-\varphi_l)^{0.3564}D_p^{0.378}\left(\frac{D_p\rho_{oil}}{\mu_{oil}}\right)^{0.09}[g(s-1)]^{0.545}}. \tag{12}$$

Under the action of the oil phase slip, the aggregate suspensions larger than the particle with critical size will be affected by gravity (g), buoyancy (F_b), and lift (F_{lift}). The F_{lift} comes from the inertia effect of flow around the hydrate agglomerates caused by the momentum of the fluid and perpendicular to the flow direction [86], which can be calculated by

$$F_{lift} = 1.615\sqrt{\gamma\rho_{oil}\mu_{oil}}\left|v_{oil}-v_{hyd}\right|r_A^2, \tag{13}$$

where γ is the fluid shear rate. The equation was the balance equation of lift and bedding force when hydrate aggregates were decomposed. When the pipe inclination angle and flow shear force were constant, the lift and bedding force of the hydrate particles would increase with the increase in the particle size. However, if the size exceeded a certain size, the bedding force would be far greater than the lift force and the hydrate would have bed deposition. In addition, when the hydrate agglomerate rased, it received resistance from the opposite direction to that of movement of aggregate relative to the fluid, which was called fluid friction F_D, which can be calculated by [87]

$$F_D = \frac{C_d\rho_{oil}\pi r_A^2}{2}\left|v_{oil}-v_{hyd}\right|^2, \tag{14}$$

where C_d is the drag coefficient, which is treated to be

constant for simplicity. It should be noted that the fluid frictional force taken into consideration was the resistance against the direction of gravity and the bedding force when the hydrate aggregates fell. The horizontal resistance is not considered because the flow friction force in the horizontal direction had little effect on the bedding force. In summary, the bedding speed and the lifting speed can be obtained, and combined with the two behaviors of hydrate lifting and bedding. The equation for the bedding rate (ψ) of hydrate aggregates was synthesized as

$$v_{\text{bedding}} = \sqrt{\frac{8r_{\text{A}}(\rho_{\text{hyd}} - \rho_{\text{oil}})g\sin\theta}{3\rho_{\text{oil}}C_{\text{d}}}}, \tag{15}$$

$$v_{\text{lift}} = \sqrt{\frac{2F_{\text{lift}}}{\rho_{\text{oil}}C_{\text{d}}\pi r_{\text{A}}^2}}, \tag{16}$$

$$\psi = \frac{\rho_{\text{hyd}}(v_{\text{bedding}}\alpha_{\text{hyd/oil}} - v_{\text{lift}}\alpha_{\text{hyd/bed}})A_{\text{bed}}}{V_{\text{CV}}}, \tag{17}$$

where C_{d} is the drag coefficient, for simplicity, it can be considered as a constant [88], with a value of 0.47 for rough spheres; $\alpha_{\text{hyd/oil}}$ and $\alpha_{\text{hyd/bed}}$ are the volume fractions of hydrate agglomerates in the oil layer and bed layer, respectively; A_{bed} is the surface area of the bed in a pipe section; and V_{CV} is the volume of the pipe section.

5.2 Quantitative model of hydrate blockage risk

The quantification of the risk of hydrate blockage in a liquid-rich system is the key and core of the prevention and control of hydrate blockage based on theoretical knowledge. However, due to the difference in system parameters and steady-state conditions between the static reactor and the experimental loop, and the gap with the pilot-scale pipeline, the quantification of the risk of hydrate blockage still has theoretical flaws.

Zerpa et al. [89] quantified the risk of hydrate blockage based on pressure drop, hydrate volume fraction, and relative viscosity, but this method was limited to fluids with specific geometric shapes. Kinnari et al. [81] based on Statoil's adapted hydrate kinetics technology to assess the risk of hydrate blockage through induction time, hydrate transportability, water content, and related parameter information of the pipeline. Wang et al. [90] proposed tetrahydrofuran (THF) and hydrochlorofluorocarbon-141b (HCFC-141b) hydrate risk assessment and prediction models based on non-dimensional parameters, which evaluated the effect of fluid kinetic energy on the agglomeration and separation tendency of hydrate particles. The dimensionless parameters were given by

$$C_{\text{h}} = \frac{\rho_{\text{mix}}v_{\text{mix}}^2/2}{6d_{\text{pipe}}\Phi_{\text{cril}}\tau/d_{\text{particle}}}, \tag{18}$$

where d_{pipe} is the diameter of the pipe, ρ_{mix} is the density of the mixture, Φ_{cril} is the critical concentration of the hydrate particles in the system, of which a sudden increase in pressure drop is observed, d_{particle} is the diameter of hydrate monomer/aggregate, v_{mix} is the mixing speed, and τ is the sum of cohesion, which can be used in the form of yield stress and can be obtained from pressure drop data. Although this model can predict the risk of hydrate and quantify the flow guarantee safety, it is difficult to obtain reliable yield stress values of natural gas hydrate formations. In addition, due to the lack of consideration of interface characteristics, it is impossible to apply this model to other fluids.

Based on the Buckingham-Pi theorem, Chaudhari et al. [91] determined the dimensionless number that played a key role in the transition of hydrate blockage risk. The results showed that the transformation to a system mainly depended on the Reynolds number and the number of capillaries [32]:

$$\frac{\Phi_{\text{hyd,transition}}}{\Phi_{\text{hyd,packing}}} = k_0 Re^{\alpha} Ca^{\beta}, \tag{19}$$

where Ca is the capillary number; Re is the Reynolds number of the continuous phase, which is oil in the case of an oil-dominated system; $\Phi_{\text{hyd,transition}}$ is the hydrate volume fraction when the hydrate risk transits from low to medium or high hydrate blockage risk area; $\Phi_{\text{hyd,packing}}$ is the volume fraction of packing hydrate, assumed to be 0.52; and k_0, α, and β are constants involved in the correlation, which can be obtained after linear regression analysis of experimental data. Therefore, Chaudhari et al. obtained the Eq. (20) after linear regression analysis.

$$\frac{\Phi_{\text{hyd,transition}}}{\Phi_{\text{hyd,packing}}} = 0.02[Re(1-LL)]^{0.52}Ca^{0.27}, \tag{20}$$

where LL is the liquid load of the system. Combining the relevant parameters of the experiment with extended dimensionless numbers (Re and Ca) by their definition, they developed the hydrate risk evaluator (HRE) index

$$\text{HRE} = 500\frac{\dfrac{\Phi_{\text{hydrate}}/1-\Phi_{\text{hydrate}}}{LL}}{\left[\left(\dfrac{\rho_{\text{oil}}v_{\text{mix}}d_{\text{pipe}}}{\mu_{\text{oil}}}\right)(1-LL)\right]^{0.52}\left(\dfrac{\mu_{\text{oil}}v_{\text{oil}}}{\sigma_{\text{oil-water}}}\right)^{0.27}}, \tag{21}$$

where Φ_{hydrate} is the volume fraction of hydrate, and $\sigma_{\text{oil-water}}$ is standard deviation. The HRE index is a function of the number of hydrates formation. It should be noted that the HRE index was based on and only applicable to oil continuous systems, and was not be applicable in water-dominated or PD systems. Moreover, the deposition effect caused by the growth of the hydrate tube wall film was ignored in the calculation process.

5.3 Pressure drop model of rich liquid system

In order to better characterize the flow behavior and

stability of the hydrate slurry, it is necessary to introduce the pressure drop curve during the slurry flow. Therefore, it is important to model the pressure drop to estimate the energy loss in the flow process. Chen et al. [92], combining the hydrate flow rate and pressure drop under the bubbly flow condition of the water-dominant system, characterized the resistance characteristics of the first hydrate formation and the start-up process, and predicted the hydrate formation, aggregation, deposition, and uniformity of particle distribution based on the rising and falling of the flow velocity and pressure drop. In general, the more stable the pressure drop with time, the higher the flow stability of the hydrate slurry. The most classic calculation of pressure drop is the Darcy-Weisbach equation [93]

$$\Delta P = \rho g h = \lambda \frac{L}{D} \frac{\rho V^2}{2}, \tag{22}$$

where ρ is the density of the mixture, g is the acceleration due to gravity, h is head loss of the test section; L is length of the test section, D is the inner diameter of the test section, V is the velocity of the flowing mixture in the test section, and λ is the friction coefficient. However, because the collision, aggregation, and decomposition of aggregates between hydrate particles generally exist in the gas-liquid system, the total friction coefficient is divided into the hydraulic friction coefficient (λ_1) of the liquid when there is no hydrate, the additional friction coefficient (λ_2) affected by hydrate aggregation, and the friction coefficient (λ_3) owing to the effect between the hydrate particles and the liquid phase. Therefore, the pressure drop of the hydrate slurry flow is expressed as [92]

$$\Delta P = (\lambda_1 + \lambda_2 + \lambda_3) \frac{L}{D} \frac{\rho_w V^2}{2}. \tag{23}$$

For the first type of friction coefficient, first, determine the low state according to the calculation of the Reynolds number. The calculation equation of the Reynolds number is

$$Re_{\mathrm{L}} = \frac{\rho_{\mathrm{w}} V D}{\mu_{\mathrm{w}}}, \tag{24}$$

$$Re_1 = \frac{2e}{D}, \tag{25}$$

where ρ_{w} is the density of water, μ_{w} is the kinematic viscosity of water, e is the absolute equivalent roughness of the pipe, Re_{L} is the Reynolds number of the liquid carrier, and Re_1 is the critical Reynolds number at which the pipe flow changes from laminar flow to turbulent flow. The critical Reynolds number for the transition from laminar flow to turbulent flow is 3000, and the critical Reynolds number when pipe flow changes from a hydraulically smooth zone to a transition zone is 27065. Here taking the hydraulically smooth zone as an example, λ_1 can be calculated using the Blasius equation

$$\lambda_1 = \frac{0.3164}{Re_{\mathrm{L}}^{0.25}}. \tag{26}$$

For the second type of friction coefficient, combining the shear force on the tube wall caused by the action of hydrate particles and the Darcy-Weisbach formula, the hydrate force balance can be used to obtain the friction coefficient λ_2 caused by the aggregation of hydrate particles, specifically expressed as

$$\lambda_2 = \frac{8}{V^2} \frac{\rho_{\mathrm{s}}}{\rho_{\mathrm{w}}} d_{\mathrm{p}}^2 f(\varphi) \gamma_{w,t}^2, \tag{27}$$

where ρ_{s} is the density of methane gas hydrate particles, $f(\varphi)$ is the function of hydrate volume fraction, d_{p} is the diameter of hydrate particles or aggregates, and $\gamma_{w,t}$ is the shear rate of the turbulent wall. Assuming ignoring the non-Newtonian behavior of hydrate slurry, combining the turbulent shear rate equation and the wall shear force equation based on the definition of the friction coefficient caused by the liquid, the expression of the shear rate can be obtained as

$$\gamma_{w,t} = \frac{\frac{f}{16}}{\frac{}{Re_{\mathrm{L}}}} \frac{8V}{D} = C_{\mathrm{f}} \frac{8V}{D}, \tag{28}$$

where f is the Fanning coefficient of friction and C_{f} is the correction coefficient for the shear rate. Therefore, the additional friction factor caused by hydrate formation and aggregation can be obtained as

$$\lambda_2 = 512 C_{\mathrm{f}}^2 \frac{\rho_{\mathrm{s}}}{\rho_{\mathrm{w}}} \left(\frac{d_{\mathrm{p}}}{D}\right)^2 f(\varphi) = g(Re_{\mathrm{L}}) \frac{\rho_{\mathrm{s}}}{\rho_{\mathrm{w}}} \left(\frac{d_{\mathrm{p}}}{D}\right)^2 f(\varphi), \tag{29}$$

where $g(Re_{\mathrm{L}})$ is a factor affected by the Reynolds number of the liquid carrier. In addition, it is of great significance to determine the relationship between $f(\varphi)$ and the calculated hydrate volume fraction. According to the Camargo-Palermo viscosity model [94], which treats hydrate aggregates as complex structures, the complex structure increases the effective volume fraction of hydrate aggregates, which can be expressed as

$$f(\varphi) = \varphi \left(\frac{d_{\mathrm{p}}}{d_0}\right)^{3-f_{\mathrm{r}}}, \tag{30}$$

where d_0 is the initial diameter of hydrate particles and f_{r} is the fractal dimension of hydrate aggregates. According to the more compact structure of the aggregate, fractal dimensions range from 2 to 2.7 under shear conditions [95], and are usually regarded as 2.5 [59]. The determination of the liquid-hydrate friction coefficient λ_3 can be calculated based on the energy loss caused by the friction between the hydrate and the liquid [96].

$$\varnothing = F\sigma\xi N = 18\rho_{\mathrm{w}}\varphi\left[\left(\frac{\varphi_{\max}}{\varphi}\right)^{\frac{1}{3}}-1\right](1-\varphi)^{-1.32}\left[\frac{(s-1)^3}{s+0.5}\right]^{0.25}Re_{\mathrm{s}}^{2.5}\frac{\upsilon_{\mathrm{w}}^3}{D^4}, \tag{31}$$

where F is the local resistance imposed by the turbulent vortex, $\varnothing$ is the energy dissipation rate due to the friction between hydrates and the liquid carrier, σ is the average length of the hydrate when it moves freely in the turbulent vortex, ξ is the average frequency of turbulent fluctuations [96], N is the numerical volume fraction of hydrate per unit volume, Re_{s} is the local Reynolds number of the hydrate particles, and $\varphi_{\max}$ is the maximum packing volume fraction, which takes 5.7 here. The liquid-hydrate friction coefficient (λ_3) can be calculated using

$$\lambda_3 = \frac{2D\varnothing}{\rho_{\mathrm{sl}}V^3} = 36\frac{\rho_{\mathrm{w}}}{\rho_{\mathrm{sl}}}\varphi\left[\left(\frac{\varphi_{\max}}{\varphi}\right)^{\frac{1}{3}}-1\right](1-\varphi)^{-1.32}\left[\frac{(s-1)^3}{s+0.5}\right]^{0.25}Re_{\mathrm{s}}^{2.5}\frac{\upsilon_{\mathrm{w}}^3}{V^3D^3}, \tag{32}$$

where ρ_{sl} is the density of the hydrate slurry and υ_{w} is the kinematic viscosity of water. Finally, the prediction model of the total pressure drop can be derived, expressed as

$$\Delta P = \left[\frac{0.3164}{Re_L^{0.25}} + g(Re_L)s\left(\frac{d_{\mathrm{p}}}{D}\right)^2\varphi\left(\frac{d_{\mathrm{p}}}{d_0}\right)^{3-f_r} + 36\frac{\rho_w}{\rho_{\mathrm{sl}}}\varphi\left[\left(\frac{\varphi_{\max}}{\varphi}\right)^{\frac{1}{3}}-1\right](1-\varphi)^{-1.32}\left[\frac{(s-1)^3}{s+0.5}\right]^{0.25}Re_{\mathrm{s}}^{2.5}\frac{\upsilon_{\mathrm{w}}^3}{V^3D^3}\right]\frac{\rho_{\mathrm{w}}LV^2}{2D}. \tag{33}$$

Because there are few research reports on hydrate plugging in PD systems, there is a lack of relevant hydrate slurry models to help understand the mechanism of hydrate flow behavior in this system. At present, hydrate research in gas dominant systems and water dominant systems has become mature [97–99]. Therefore, the establishment of a comprehensive model for hydrate pipe plugging in a PD system may be the focus of future research.

6 Conclusions and perspectives

6.1 Conclusions

Liquid-rich systems in a gathering pipeline can be divided into oil-based systems, water-based systems, and PD systems. The mechanism of hydrate pipe plugging in oil-based systems is diversified, mainly including accumulation, implantation deposition, and wall adhesion of hydrate. In water-based systems, the growth rate of hydrates is low and the risk of pipe blockage is the lowest in all systems. The pipe blockage mechanism is dominated by the implantation and deposition of hydrate particles and affected by the emulsification state and oil-water dispersion. The hydrate blockage mechanism in PD systems is hydrate film growth and tube wall adhesion, which mainly depend on the temperature difference between the fluid, the wall, and the gas solubility in the bulk phase. The formation of hydrate in a PD system would lead to the occurrence of migration at the oil-water interface, which increases the tendency of hydrate to block pipes. The flow rate and water content in an oil-water two-phase system would have a certain impact on oil-water dispersion state, friction coefficient, pressure drop, fluid flow pattern, hydrate slurry viscosity, and hydrate formation rate in the system.

6.2 Future research perspectives

At present, influence of water content and flow velocity in the system on the mechanism and risk of blocking is still in the research stage. Combining the current experimental research status of hydrate slurry flow characteristic and hydrate blockage mechanism under a flow system, several suggestions can be proposed.

There is a general lack of reports on the results of microscopic instrumentality in current research loop experiments. Experimental studies of microscopic behavior of hydrates, such as hydrate nucleation growth, aggregation between particles, and hydrate deposition, are necessary to combine specific parameter changes and microscopic phenomena for in-depth analysis to reinforce the persuasiveness and accuracy of the experiment. At the same time, it is essential to establish a comprehensive hydrate blockage model to predict the process of hydrate blockage.

There is currently no rationalization for the oil-water demulsification in water-based systems and migration of oil-water interfaces in PD systems. Moreover, there is no corresponding microscopic experiment to confirm the phenomenon that the free water phase in the solution would affect the oil-water dispersion state in rich-liquid systems and thus affect the hydrate blockage mechanism. Research on the formation and blockage of hydrates in PD systems is still in its infancy. Therefore, scholars should continue to strengthen the mastery of theoretical knowledge of the clogging mechanism of this system.

Most of the hydrate loop experimental research are devoted to the hydrate formation in straight pipelines, but the theoretical knowledge on hydrate formation in special environments such as bends, valves, and dead angle is relatively scarce and lacking. Although several scholars used simulation software of fluid dynamics to conduct research in this field, there was a scarcity of comparison between actual experimental data that can enhance accuracy and practicability. Therefore, the characteristics

of hydrate formation in special environments except for straight pipelines should be the next research hotspot.

The present paper has principally explored the influence of water content and flow rate factors on hydrate blockage. The effect of other factors such as particle size, gas-liquid ratio, kinetic inhibitors and anti-polymerization agents on hydrate accumulation and deposition and blockage should also be studied in-depth. Additionally, a quantitative analysis of the effect of each factor on the risk of pipe blockage should be conducted. The proficiency in these theories can improve the practical application of guaranteeing the transportation of hydrate slurry by controlling external conditions.

Up to the present, most loop devices are opaque or have only a single window, which is not convenient for observing the fluid flow behavior in the whole loop. It is necessary to development a fully visualized flow loop experimental device that can demonstrate flow patterns and flow characteristics of any part of the loop test section. Through these improvements, scholars can more deeply understand the influence of hydrate accumulation and deposition on the flow stability of hydrate slurry. More and greater breakthroughs of improvements and upgrades to flow loop devices are still expected.

Acknowledgments This work was supported by the Doctoral Research Start-up Fund Project of Liaoning Province (2019-BS-159), the Scientific Research Fund Project of Liaoning Education Department (L2019024), and the Key Scientific Research Project of Liaoning Provincial Department of Education (L2020002).

References

1. Gaurav B, Goh M N, Arumuganainar S E K, et al. Ultra-rapid uptake and the highly stable storage of methane as combustible ice. Energy and Environmental Science, 2020, 13(12): 4946–4961
2. Song S, Shi B, Yu W, et al. Study on the optimization of hydrate management strategies in deepwater gas well testing operations. Journal of Energy Resources Technology, 2020, 142(3): 033002
3. Shi G, Song S, Shi B, et al. A new transient model for hydrate slurry flow in oil-dominated flowlines. Journal of Petroleum Science and Engineering, 2021, 196: 108003
4. Shi B, Song S, Chen Y, et al. Status of natural gas hydrate flow assurance research in China: a review. Energy and Fuels, 2021, 35(5): 3611–3658
5. Song S, Shi B, Yu W, et al. A new methane hydrate decomposition model considering intrinsic kinetics and mass transfer. Chemical Engineering Journal, 2019, 361: 1264–1284
6. Hao W, Wang J, Fan S, et al. Evaluation and analysis method for natural gas hydrate storage and transportation processes. Energy Conversion and Management, 2008, 49(10): 2546–2553
7. Veluswamy H P, Kumar R, Linga P. Hydrogen storage in clathrate hydrates: current state of the art and future directions. Applied Energy, 2014, 122: 112–132
8. Kubota H, Shimizu K, Tanaka Y, et al. Thermodynamic properties of R13 ($CClF_3$), R23 (CHF_3), R152a ($C_2H_4F_2$), and propane hydrates for desalination of sea water. Journal of Chemical Engineering of Japan, 1984, 17(4): 423–429
9. Yang M, Song Y, Jiang L, et al. Effects of operating mode and pressure on hydrate-based desalination and CO_2 capture in porous media. Applied Energy, 2014, 135: 504–511
10. Cai J, Xu C, Xia Z, et al. Hydrate-based methane separation from coal mine methane gas mixture by bubbling using the scale-up equipment. Applied Energy, 2017, 204: 1526–1534
11. Zhong D, Ding K, Lu Y, et al. Methane recovery from coal mine gas using hydrate formation in water-in-oil emulsions. Applied Energy, 2016, 162: 1619–1626
12. Xie N, Tan C, Yang S, et al. Conceptual design and analysis of a novel CO_2 hydrate-based refrigeration system with cold energy storage. ACS Sustainable Chemistry and Engineering, 2019, 7(1): 1502–1511
13. Liu Z, Liu W, Lang C, et al. Viscosity investigation on metastable hydrate suspension in oil-dominated systems. Chemical Engineering Science, 2021, 238: 116608
14. Li X, Xu C, Chen Z, et al. Tetra-*n*-butyl ammonium bromide semi-clathrate hydrate process for post-combustion capture of carbon dioxide in the presence of dodecyl trimethyl ammonium chloride. Energy, 2010, 35(9): 3902–3908
15. Li X, Xu C, Chen Z, et al. Hydrate-based pre-combustion carbon dioxide capture process in the system with tetra-*n*-butyl ammonium bromide solution in the presence of cyclopentane. Energy, 2011, 36(3): 1394–1403
16. Hammerschmidt E G. Formation of gas hydrates in natural gas transmission lines. Industrial and Engineering Chemistry, 1934, 26(8): 851–855
17. Stern L A, Circone S, Kirby S H, et al. Temperature, pressure, and compositional effects on anomalous or “self” preservation of gas hydrates. Canadian Journal of Physics, 2003, 81(1−2): 271–283
18. Lv X, Zuo J, Liu Y, et al. Experimental study of growth kinetics of CO_2 hydrates and multiphase flow properties of slurries in high pressure flow systems. RSC Advances, 2019, 9(56): 32873–32888
19. Yang M, Song Y, Ruan X, et al. Characteristics of CO_2 hydrate formation and dissociation in glass beads and silica gel. Energies, 2012, 5(4): 925–937
20. Zhang H, Du J, Wang Y, et al. Investigation into THF hydrate slurry flow behaviour and inhibition by an anti-agglomerant. RSC Advances, 2018, 8(22): 11946–11956
21. Merlin F, Guitouni H, Mouhoubi H, et al. Adsorption and heterocoagulation of nonionic surfactants and latex particles on cement hydrates. Journal of Colloid and Interface Science, 2005, 281(1): 1–10
22. Aman Z M, Koh C A. Interfacial phenomena in gas hydrate systems. Chemical Society Reviews, 2016, 45(6): 1678–1690
23. Wang F, Chen P, Li X, et al. Effect of colloidal silica on the hydration behavior of calcium aluminate cement. Materials, 2018, 11(10): 1849
24. Song S, Liu Z, Zhou L, et al. Research progress on hydrate plugging in multiphase mixed rich-liquid transportation pipelines. Frontiers in Energy, 2020, online, https://doi.org/10.1007/s11708-020-0688-x

25. Joshi S V, Grasso G A, Lafond P G, et al. Experimental flowloop investigations of gas hydrate formation in high water cut systems. Chemical Engineering Science, 2013, 97: 198–209
26. Fidel-Dufour A, Gruy F, Herri J M. Rheology of methane hydrate slurries during their crystallization in a water in dodecane emulsion under flowing. Chemical Engineering Science, 2006, 61(2): 505–515
27. van der Hofstadt M, Fabregas R, Millan-Solsona R, et al. Internal hydration properties of single bacterial endospores probed by electrostatic force microscopy. ACS Nano, 2016, 10(12): 11327–11336
28. Taylor C J, Dieker L E, Miller K T, et al. Micromechanical adhesion force measurements between tetrahydrofuran hydrate particles. Journal of Colloid and Interface Science, 2007, 306(2): 255–261
29. Yang S O, Kleehammer D M, Huo Z, et al. Temperature dependence of particle-particle adherence forces in ice and clathrate hydrates. Journal of Colloid and Interface Science, 2004, 277(2): 335–341
30. Orr F M, Scriven L E, Rivas A P. Pendular rings between solids: meniscus properties and capillary force. Journal of Fluid Mechanics, 1975, 67(4): 723–742
31. Liu C, Zhang C, Zhou C, et al. Effects of the solidification of capillary bridges on the interaction forces between hydrate particles. Energy and Fuels, 2020, 34(4): 4525–4533
32. Aman Z M, Brown E P, Sloan E D, et al. Interfacial mechanisms governing cyclopentane clathrate hydrate adhesion/cohesion. Physical Chemistry Chemical Physics, 2011, 13(44): 19796–19806
33. Palermo T, Fidel-Dufour A, Maurel P, et al. Model of hydrates agglomeration–application to hydrates formation in an acidic crude oil. In: 12th International Conference on Multiphase Production Technology, Barcelona, Spain, 2005
34. Shi B, Ding L, Li W, et al. Investigation on hydrates blockage and restart process mechanisms of CO_2 hydrate slurry flow. Asia-Pacific Journal of Chemical Engineering, 2018, 13(3): e2193
35. Liu Z, Vasheghani Farahani M, Yang M, et al. Hydrate slurry flow characteristics influenced by formation, agglomeration and deposition in a fully visual flow loop. Fuel, 2020, 277: 118066
36. Aspenes G, Dieker L E, Aman Z M, et al. Adhesion force between cyclopentane hydrates and solid surface materials. Journal of Colloid and Interface Science, 2010, 343(2): 529–536
37. Balakin B V, Hoffmann A C, Kosinski P, et al. Turbulent flow of hydrates in a pipeline of complex configuration. Chemical Engineering Science, 2010, 65(17): 5007–5017
38. Hernandez O C. Investigation of hydrate slurry flow in horizontal pipelines. Dissertation for the Doctoral Degree. Tulsa: The University of Tulsa, 2006
39. Kwak G H, Lee K, Lee B R, et al. Quantification of the risk for hydrate formation during cool down in a dispersed oil-water system. Korean Journal of Chemical Engineering, 2017, 34(7): 2043–2048
40. Aman Z M, Leith W J, Grasso G A, et al. Adhesion force between cyclopentane hydrate and mineral surfaces. Langmuir: the ACS Journal of Surfaces and Colloids, 2013, 29(50): 15551–15557
41. Doron P, Simkhis M, Barnea D. Flow of solid-liquid mixtures in inclined pipes. International Journal of Multiphase Flow, 1997, 23(2): 313–323
42. Grasso G. Investigation of hydrate formation and transportability in multiphase flow systems. Dissertation for the Doctoral Degree. Golden: Colorado School of Mines, 2015
43. Hu S, Kim T H, Park J G, et al. Effect of different deposition mediums on the adhesion and removal of particles. Journal of the Electrochemical Society, 2010, 157(6): H662
44. Turner D J. Clathrate hydrate formation in water-in-oil dispersions. Dissertation for the Doctoral Degree. Golden: Colorado School of Mines, 2005
45. Turner D J, Miller K T, Sloan E D. Methane hydrate formation and an inward growing shell model in water-in-oil dispersions. Chemical Engineering Science, 2009, 64(18): 3996–4004
46. Taylor C J, Miller K T, Koh C A, et al. Macroscopic investigation of hydrate film growth at the hydrocarbon/water interface. Chemical Engineering Science, 2007, 62(23): 6524–6533
47. Sum A K, Koh C A, Sloan E D. Developing a comprehensive understanding and model of hydrate in multiphase flow: from laboratory measurements to field applications. Energy and Fuels, 2012, 26(7): 4046–4052
48. Ding L, Shi B, Wang J, et al. Hydrate deposition on cold pipe walls in water-in-oil (W/O) emulsion systems. Energy and Fuels, 2017, 31(9): 8865–8876
49. Song G, Li Y, Wang W, et al. Investigation of hydrate plugging in natural gas+diesel oil+water systems using a high-pressure flow loop. Chemical Engineering Science, 2017, 158: 480–489
50. Akhfash M, Boxall J A, Aman Z M, et al. Hydrate formation and particle distributions in gas-water systems. Chemical Engineering Science, 2013, 104: 177–188
51. Majid A A, Lee W, Srivastava V, et al. Experimental investigation of gas-hydrate formation and particle transportability in fully and partially dispersed multiphase-flow systems using a high-pressure flow loop. SPE Journal, 2018, 23(3): 937–951
52. Sloan D, Koh C, Sum A K, et al. Natural Gas Hydrates in Flow Assurance. Burlington: Gulf Professional Publishing, 2010
53. Majid A A, Lee W, Srivastava V, et al. The study of gas hydrate formation and particle transportability using a high pressure flowloop. In: Offshore Technology Conference, Houston, Texas, USA, 2016
54. Vijayamohan P. Experimental investigation of gas hydrate formation, plugging and transportability in partially dispersed and water continuous systems. Dissertation for the Doctoral Degree. Golden: Colorado School of Mines, 2015
55. Akhfash M, Aman Z M, Ahn S Y, et al. Gas hydrate plug formation in partially-dispersed water-oil systems. Chemical Engineering Science, 2016, 140: 337–347
56. Arjmandi M, Tohidi B, Danesh A, et al. Is subcooling the right driving force for testing low-dosage hydrate inhibitors? Chemical Engineering Science, 2005, 60(5): 1313−1321
57. Vysniauskas A, Bishnoi P R. A kinetic study of methane hydrate formation. Chemical Engineering Science, 1983, 38(7): 1061–1072
58. Lv X F, Shi B H, Wang Y, et al. Experimental study on hydrate induction time of gas-saturated water-in-oil emulsion using a

high-pressure flow loop. Oil and Gas Science and Technology – Revue d'IFP Energies Nouvelles, 2015, 70(6): 1111–1124
59. Liu Y, Shi B, Ding L, et al. Investigation of hydrate agglomeration and plugging mechanism in low-wax-content water-in-oil emulsion systems. Energy and Fuels, 2018, 32(9): 8986–9000
60. Peytavy J L, Monfort J P, Gaillard C. Investigation of methane hydrate formation in a recirculating flow loop: modeling of the kinetics and tests of efficiency of chemical additives on hydrate inhibition. Oil and Gas Science and Technology, 1999, 54(3): 365–374
61. Lv X, Shi B, Wang Y, et al. Study on gas hydrate formation and hydrate slurry flow in a multiphase transportation system. Energy and Fuels, 2013, 27(12): 7294–7302
62. Zhang S, Pan Z, Shang L, et al. Analysis of influencing factors on the kinetics characteristics of carbon dioxide hydrates in high pressure flow systems. Energy and Fuels, 2021, 35(19): 16241–16257
63. Urdahl O, Lund A, Mørk P, et al. Inhibition of gas hydrate formation by means of chemical additives—I. Development of an experimental set-up for characterization of gas hydrate inhibitor efficiency with respect to flow properties and deposition. Chemical Engineering Science, 1995, 50(5): 863–870
64. Andersson V, Gudmundsson J S. Flow properties of hydrate-in-water slurries. Annals of the New York Academy of Sciences, 2006, 912(1): 322–329
65. Lachance J W, Talley L D, Shatto D P, et al. Formation of hydrate slurries in a once-through operation. Energy and Fuels, 2012, 26(7): 4059–4066
66. Talaghat M R. Experimental investigation of induction time for double gas hydrate formation in the simultaneous presence of the PVP and l-Tyrosine as kinetic inhibitors in a mini flow loop apparatus. Journal of Natural Gas Science and Engineering, 2014, 19: 215–220
67. Melchuna A, Cameirão A, Ouabbas Y, et al. Transport of hydrate slurry at high water cut. In: The 8 th International Conference on Gas Hydrates, Beijing, China, 2014
68. Vijayamohan P, Majid A, Chaudhari P, et al. Hydrate modeling & flow loop experiments for water continuous & partially dispersed systems. In: Offshore Technology Conference, Houston, Texas, USA, 2014
69. Ding L, Shi B, Lv X, et al. Hydrate formation and plugging mechanisms in different gas-liquid flow patterns. Industrial and Engineering Chemistry Research, 2017, 56(14): 4173–4184
70. Clain P, Delahaye A, Fournaison L, et al. Rheological properties of tetra-*n*-butylphosphonium bromide hydrate slurry flow. Chemical Engineering Journal, 2012, 193–194: 112−122
71. Peng B, Chen J, Sun C, et al. Flow characteristics and morphology of hydrate slurry formed from (natural gas+diesel oil/condensate oil+water) system containing anti-agglomerant. Chemical Engineering Science, 2012, 84: 333–344
72. Yan K, Sun C, Chen J, et al. Flow characteristics and rheological properties of natural gas hydrate slurry in the presence of anti-agglomerant in a flow loop apparatus. Chemical Engineering Science, 2014, 106: 99–108
73. Shi B, Ding L, Liu Y, et al. Hydrate slurry flow property in W/O emulsion systems. RSC Advances, 2018, 8(21): 11436–11445
74. Srivastava V, Eaton M W, Koh C A, et al. Quantitative framework for hydrate bedding and transient particle agglomeration. Industrial and Engineering Chemistry Research, 2020, 59(27): 12580–12589
75. Liu W, Hu J, Li X, et al. Assessment of hydrate blockage risk in long-distance natural gas transmission pipelines. Journal of Natural Gas Science and Engineering, 2018, 60: 256–270
76. Rao I, Koh C A, Sloan E D, et al. Gas hydrate deposition on a cold surface in water-saturated gas systems. Industrial and Engineering Chemistry Research, 2013, 52(18): 6262–6269
77. di Lorenzo M, Aman Z M, Kozielski K, et al. Underinhibited hydrate formation and transport investigated using a single-pass gas-dominant flowloop. Energy and Fuels, 2014, 28(11): 7274–7284
78. Ding L, Shi B, Lv X, et al. Hydrate formation and plugging mechanisms in different gas-liquid flow patterns. Industrial & Engineering Chemistry Research, 2017, 56(14): 4173–4184
79. Ding L, Shi B, Liu Y, et al. Rheology of natural gas hydrate slurry: effect of hydrate agglomeration and deposition. Fuel, 2019, 239: 126–137
80. Davies S R, Boxali J A, Koh C A, et al. Predicting hydrate-plug formation in a subsea tieback. SPE Production and Operations, 2009, 24(4): 573–578
81. Kinnari K, Hundseid J, Li X, et al. Hydrate management in practice. Journal of Chemical and Engineering Data, 2015, 60(2): 437–446
82. Charlton T B, di Lorenzo M, Zerpa L E, et al. Simulating hydrate growth and transport behavior in gas-dominant flow. Energy and Fuels, 2018, 32(2): 1012–1023
83. Moradpour H, Chapoy A, Tohidi B. Bimodal model for predicting the emulsion-hydrate mixture viscosity in high water cut systems. Fuel, 2011, 90(11): 3343–3351
84. Liu X, Flemings P B. Dynamic multiphase flow model of hydrate formation in marine sediments. Journal of Geophysical Research, 2007, 112(B3): B03101
85. Oroskar A R, Turian R M. The critical velocity in pipeline flow of slurries. AIChE Journal, 1980, 26(4): 550–558
86. Boxall J A, Koh C A, Sloan E D, et al. Droplet size scaling of water-in-oil emulsions under turbulent flow. Langmuir: the ACS Journal of Surfaces and Colloids, 2012, 28(1): 104–110
87. Saffman P G. The lift on a small sphere in a slow shear flow. Journal of Fluid Mechanics, 1965, 22(2): 385–400
88. Richter A, Nikrityuk P A. Drag forces and heat transfer coefficients for spherical, cuboidal and ellipsoidal particles in cross flow at sub-critical Reynolds numbers. International Journal of Heat and Mass Transfer, 2012, 55(4): 1343–1354
89. Zerpa L E, Sloan E D, Koh C, et al. Hydrate risk assessment and restart-procedure optimization of an offshore well using a transient hydrate prediction model. Oil and Gas Facilities, 2012, 1(5): 49–56
90. Wang W, Fan S, Liang D, et al. A model for estimating flow assurance of hydrate slurry in pipelines. Journal of Natural Gas Chemistry, 2010, 19(4): 380–384
91. Chaudhari P, Zerpa L E, Sum A K. A correlation to quantify hydrate plugging risk in oil and gas production pipelines based on

hydrate transportability parameters. Journal of Natural Gas Science and Engineering, 2018, 58: 152–161

92. Chen Y, Gong J, Shi B, et al. Investigation into methane hydrate reformation in water-dominated bubbly flow. Fuel, 2020, 263: 116691
93. Brown G O. The history of the darcy-weisbach equation for pipe flow resistance. In: American Society of Civil Engineers Environmental and Water Resources History Sessions at ASCE Civil Engineering Conference and Exposition 2002, Washington, D.C.. 2002, 34–43
94. Camargo R, Palermo T, Sinquin A, et al. Rheological characterization of hydrate suspensions in oil dominated systems. Annals of the New York Academy of Sciences, 2006, 912(1): 906–916
95. Camargo R, Palermo T. Rheological properties of hydrate suspensions in an asphaltenic crude oil. In: Proceedings of the 4th International Conference on Gas Hydrates, Yokohama, Japan, 2002
96. Eskin D, Scarlett B. Model of the solids deposition in hydrotransport: an energy approach. Industrial and Engineering Chemistry Research, 2005, 44(5): 1284–1290
97. Wu Y, Shang L, Pan Z, et al. Gas hydrate formation in the presence of mixed surfactants and alumina nanoparticles. Journal of Natural Gas Science and Engineering, 2021, 94: 104049
98. Zhang S, Shang L, Zhou L, et al. Hydrate deposition model and flow assurance technology in gas-dominant pipeline transportation systems: a review. Energy & Fuels, 2022, 36(4): 1747-1775
99. Qin Y, Shang L, Lv Z, et al. Rapid formation of methane hydrate in environment-friendly leucine-based complex system. Energy, 2022, 254: 124214